

# Annual progress report 1993. Work in controlled thermonuclear fusion research performed in the fusion research unit under the contract af association between Euratom and Risø National Laboratory

**Astradsson, L.; Jensen, Vagn Orla**

*Publication date:*
1994

*Document Version*
Publisher's PDF, also known as Version of record

RISØ

Risø-R-761(EN)

# ANNUAL PROGRESS REPORT 1993

## Work in Controlled Thermonuclear Fusion Research Performed in The Fusion Research Unit under the Contract of Association between Euratom and Risø National Laboratory

Edited by L. Astradsson and V.O. Jensen

Risø National Laboratory, Roskilde, Denmark
September 1994

# ANNUAL PROGRESS REPORT 1993

Risø-R-761(EN)

# Work in Controlled Thermonuclear Fusion Research Performed in The Fusion Research Unit under the Contract of Association between Euratom and Risø National Laboratory

Edited by L. Astradsson and V.O. Jensen

Risø National Laboratory, Roskilde, Denmark
September 1994

Abstract. The programme of the Research Unit of the Fusion Association Euratom-Risø National Laboratory covers work in fusion plasma physics and in fusion technology. The fusion plasma physics group has activities within (a) studies of nonlinear dynamical processes in magnetized plasmas, (b) development of pellet injectors for fusion experiments, and (c) development of diagnostics for fusion plasmas. The activities in technology cover radiation damage of fusion reactor materials. A summary of the activities in 1993 is presented.

ISBN 87-550-2000-3
ISSN 0106-2840

Grafisk Service · Risø · 1994

# Contents

# 1 Introduction

The activities in the Research Unit cover the two main lines:

**A) Work in the fusion plasma physics group** which includes the following topics:

- *Nonlinear dynamics of fusion plasmas*
  This research area is concerned with theoretical, numerical, and experimental investigations of nonlinear continuum systems. The main topic is nonlinear evolution of instabilities in fusion relevant plasma physics and the associated turbulent transport. The emphasis of these investigations has been on studies of coherent structures in two-dimensional flows. The nonlinear dynamic evolution of these structures, which can be characterised as localised and long-lived vortices, was studied by a combination of theoretical and numerical investigations. A detailed understanding of the physical properties of two-dimensional coherent structures is of great importance to the description of plasma confinement in magnetic fusion experiments as well as to many fundamental problems in aerodynamics and fluid dynamics.

  During 1993 the Risø Q-machine, which has been in operation since 1967 and used for experimental studies of fundamental plasma physics, was dismantled.The work also covers plasma equilibria and development of diagnostics based on coherent scattering.

- *Pellet handling, acceleration, and injection*
  A pellet injector which can inject frozen fuel pellets into fusion plasmas has been developed over the last years. The department has offered to build injectors for fusion laboratories on commercial terms. During 1993 the work has been concentrated on the construction of two systems for the Italian fusion experiments FTU in Frascati and RFX in Padova.

- *Participation in the scientific work at JET*
  This research area is concerned with studies of ELMs in the scrape off layer in JET.

**B) Work in fusion technology** which includes

- *Work on irradiation effects in materials*
- *Work on water radiolysis for NET/ITER*

# 2 Work in the Fusion Plasma Physics Group

## 2.1 Nonlinear Dynamics of Fusion Plasmas

### 2.1.1 Simulation of Viscoelastic Fluids

(Bo Gervang)

A Newtonian fluid (e.g. water) shows a linear relationship between stress and rate of deformation. The proportionality constant is the viscosity of the fluid. All other fluids are denoted non-Newtonian fluids of which the viscoelastic fluids are of particular interest in this study. These fluids behave as a Hookean solid when processed at short time scales but as a Newtonian liquid when processed at long time scales.

The flow past a sphere in an infinite expanse of fluid is simulated. This example was suggested at the Sixth International Workshop on Numerical Methods in Non-Newtonian Flow as a benchmark problem for test of different computer codes. The governing equations are discretised using spectral methods, and a domain decomposition is used in order to resolve the steep gradients in the boundary layer. Both the Eulerian and the Lagrangian formulations are tested when solving the hyperbolic stress equations. Conventional discretisation methods (finite difference, finite volume, and finite element) have only solved the equations for small values of the Deborah number whereas we can, by use of spectral methods, solve the equations for larger values of the Deborah number. The Deborah number may be interpreted as the ratio of the magnitude of the elastic forces to that of the viscous forces.

Formulating the problem in primitive variables - $\mathbf{u}, p, \mathbf{T}$ (velocity, pressure, stress) - gives rise to the solution of the time dependent Stokes operator at each time step. Optimal spaces are sought for both velocity and pressure fields in order to obtain globally solenoidal velocity fields. The associated discrete matrix is singular and new techniques are developed to solve singular systems arising from spectral discretisation of PDEs with domain decomposition.

### 2.1.2 Studies of Boundary Layer Formation and Detachment in Two-Dimensional Flows

(E.A. Coutsias (University of New Mexico, USA), J.S. Hesthaven, and J.P. Lynov)

One of the most difficult problems in industrial flow control lies in determining the effects caused by the extremely complex flow patterns generated near material boundaries. Here, boundary layers with high vorticity concentrations are usually formed, and through very irregular bursting events these boundary layers detach from the walls and enter into the main flow leading to turbulence. In most engineering designs these processes are treated in a rather crude, statistical manner. However, through the evolution of high power supercomputers and the development of new analytical and computational techniques direct and detailed studies of the fundamental flow processes near walls are beginning to be possible.

In our numerical studies of two-dimensional, wall bounded flows we have developed accurate spectral algorithms for various nonlinear, dynamic problems. During the past year several quantitative tests have been carried out in order to test the accuracy of these algorithms. One such test was the solution of the Orr-Sommerfeld equation. This is a linear eigenvalue problem which describes the onset of unstable fluctuations in a plane, pressure driven channel flow. In order to solve the eigenvalue problem, our new spectral methods described in section 2.1.3

were employed. As a result of these well-conditioned operators, we were able to determine the eigenvalues with a couple of orders of magnitude higher accuracy than those previously cited in the literature. The results from the eigenvalue problem were subsequently used to check the dynamic behaviour of our full dynamic code with excellent agreement. Similar comparisons between theoretical eigenvalue calculations and fully dynamic simulations were performed for the forced, annular shear layer problem described in section 2.1.4.

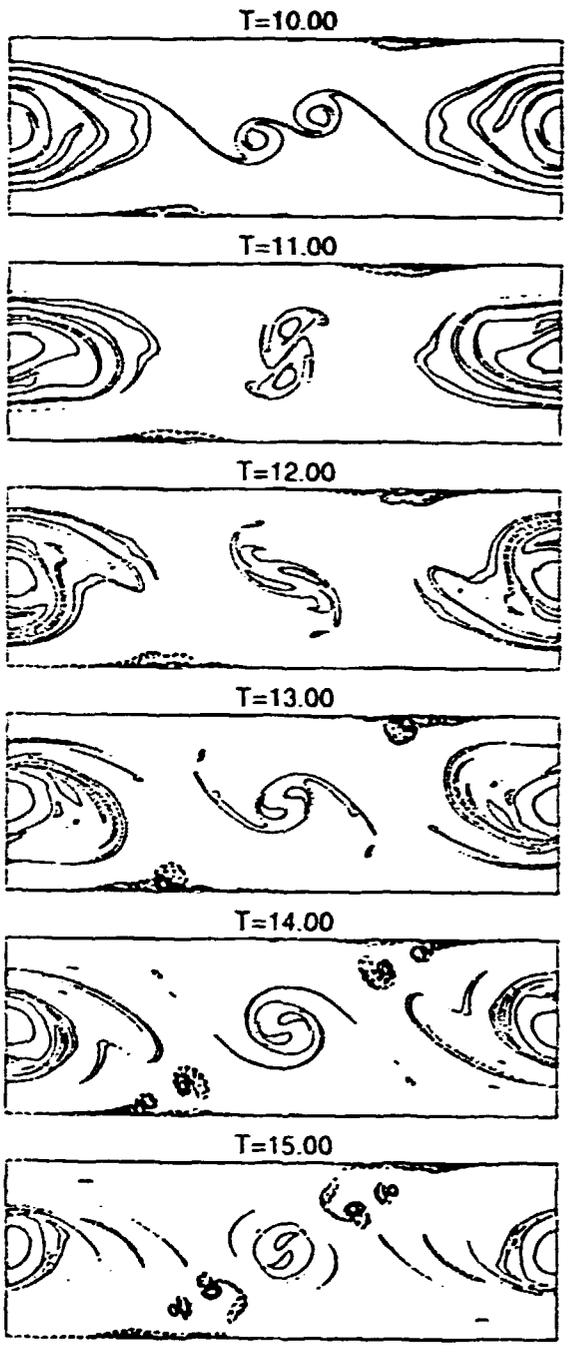


*Figure 1. Numerical simulation of shear layer roll-up in a periodic channel with oppositely moving, no-slip walls at Reynolds number 20,000.*

Theoretical studies of boundary layer evolution caused by isolated vortical structures have been initiated. The goal of these studies is to provide good, theoretical estimates of the vorticity production and boundary layer detachment caused by vortex-wall interactions. Our initial investigations have been concerned with comparisons between theoretical estimates of idealised, vortex sheet production by incoming point dipoles and the complete boundary layer formation by incoming dipoles with distributed vorticity. These studies have led to the development of new schemes for the initial projection of the vorticity field necessary in order to satisfy the no-slip boundary conditions at the walls at the very start of the simulations.

An example of complex boundary layer behaviour is shown in Fig. 1. Here results from a high resolution simulation (342 Chebyshev and 684 Fourier modes) are shown for a shear layer roll-up in a periodic channel with oppositely moving walls at Reynolds number 20,000. The contour plots show instantaneous vorticity distributions. Boundary layer formation and eruption is clearly seen when main flow vorticity approaches the channel walls.

### 2.1.3 Development of Accurate and Efficient Numerical Algorithms for the Solution of Problems with Sharp Variations

(E.A. Coutsias*, T. Hagstrom*, and D. Torres* (*University of New Mexico, USA))

The numerical studies pursued in connection with our fluid dynamics research rely critically on certain innovative algorithms that have been developed at Risø and allow the exceedingly accurate solution of boundary value problems for various differential equations.

The dynamics of vortices near walls, the filamentation occurring in the evolution of shear layers or during vortex-vortex interactions, and the analysis of flows exhibiting sharp gradients in flow properties all require the accurate integration of highly nonlinear partial differential equations for very long time. Due to the exponential instabilities and the potential occurrence of chaotic events in such problems, very high accuracy must be maintained throughout the computations.

In our efforts to maintain a very high standard of accuracy and reliability in our simulations, we have relied on the excellent approximating power of spectral families, such as Chebyshev polynomials. The general idea in these methods is the expansion of the quantities involved in terms of classical orthogonal polynomials. Then, differential operators are expressed as matrices acting on the expansion coefficients. In general, these matrices are full and ill-conditioned, and the resulting discretisation of the field equations is quite cumbersome and hard to manipulate, despite its "infinite order accuracy". Such manipulations tend to be prohibitively expensive in terms of computer time.

By taking advantage of certain simple recursion relations and other, apparently not widely known algebraic properties of orthogonal polynomials[1], we are able to solve large classes of problems, including all the problems occurring in our various hydrodynamic codes, by computationally simple and well-conditioned algorithms which scale linearly with the number of computational nodes employed in our discretisations. Several test problems that demonstrate the power of the new techniques have been solved. For example, in a problem including an internal shock wave our method allows the same accuracy to be obtained by the use of as few as 64 modes as a traditional approach would by using $\approx 32,000$ modes[2].

Special attention needs to be given to the analysis of problems in geometries involving coordinate system singularities. In this direction we have been successful in overcoming the difficulties associated with the spectral solution of the Poisson equation in a disk, an essential first step towards developing a fast and accurate

Navier-Stokes solver for flows in circular domains. This will be needed for our studies in connection with the projected parabolic rotating tank experiments that are in the construction phase at Risø.

1) Coutsias, E.A. (1993), submitted to SIAM J. of Sci. Stat. Comp.

2) Coutsias, E.A., Hagstrom, T., and Torres, D. (1993), submitted to Math. Comp.

### 2.1.4 Numerical and Analytical Studies of Transitions in Circular Shear Layers

(K. Bergeron*, E.A. Coutsias*, J.P. Lynov, and A.H. Nielsen (*University of New Mexico, USA))

The evolution of circular shear layers provides a rich backdrop for investigations of the transition to turbulence in fluids and plasmas. A better understanding of the processes involved can lead to finer methods for influencing, even controlling, this complex phenomenon. The Kelvin-Helmholtz instability of shear layers offers a generic pathway for the formation of coherent vortical structures which in recent years have become recognised as the main actors in many situations in which traditional analyses of turbulence have proved inadequate. An interesting example is offered by the problem of vortex shedding from structures that are responsible for such common phenomena as jet airplane noise, catastrophic failures of large structures under strong wind loads, and transonic flight control.

The quantisation inherent in circular geometry leads to the formation of well-defined vortical braids, unlike the incessant pairing and scale evolution of planar shear layers. Both cylindrical, magnetised, electrostatic plasma experiments and rotating fluid experiments have produced rich bifurcation sequences of different symmetries, as well as oscillating, quasi-periodic, or chaotic states. We have pursued numerical and analytical studies which demonstrate that such transitions can be accurately described by reducing the governing slightly viscous, forced Navier-Stokes equations to a system of ordinary differential equations of few degrees of freedom. The simplest case studied in detail so far leads to an equation of the Landau type describing the saturation of the Kelvin-Helmholtz instability in terms of the amplitude $A(\tau)$ of the most unstable mode, with $\tau$ a slow time scale. In this case the dynamic equation assumes the form:

$$\sigma A_\tau = \beta A + \gamma A^2 A^*.$$

The (complex) coefficients of the reduced equations are computed by numerical solution of appropriate eigenvalue problems; the resulting time evolution is in excellent agreement with direct simulations of the flow, and both sets of calculations faithfully reproduce experimental observations of circular shear layer transitions in the split annulus experiment[1].

The two approaches supplement each other in predicting the transition to states of ever increasing complexity, even beyond the regimes that have so far been experimentally accessible.

A direct practical application of this work, besides the understanding that it will produce the transition mechanism in circular shear layers, can be better understanding of flows in computer disk drives. Similar bifurcation phenomena have been observed in circular flames[2] and it will be interesting to carry out a comparison of the transition mechanisms at work in the two problems.

Ultimately, this extremely accurate reduction of the phenomenon to low dynamic system behaviour offers the promise of controlling the transitions by proper application of external forcing. An investigation of various methods of applying controlling forces to this flow is planned.

1) Chomaz et al. (1988). J. Fluid Mech. 187, 115-140.
2) Bayliss, Leaf, and Matkowsky (1993). Comb. Sci. Tech. to appear.

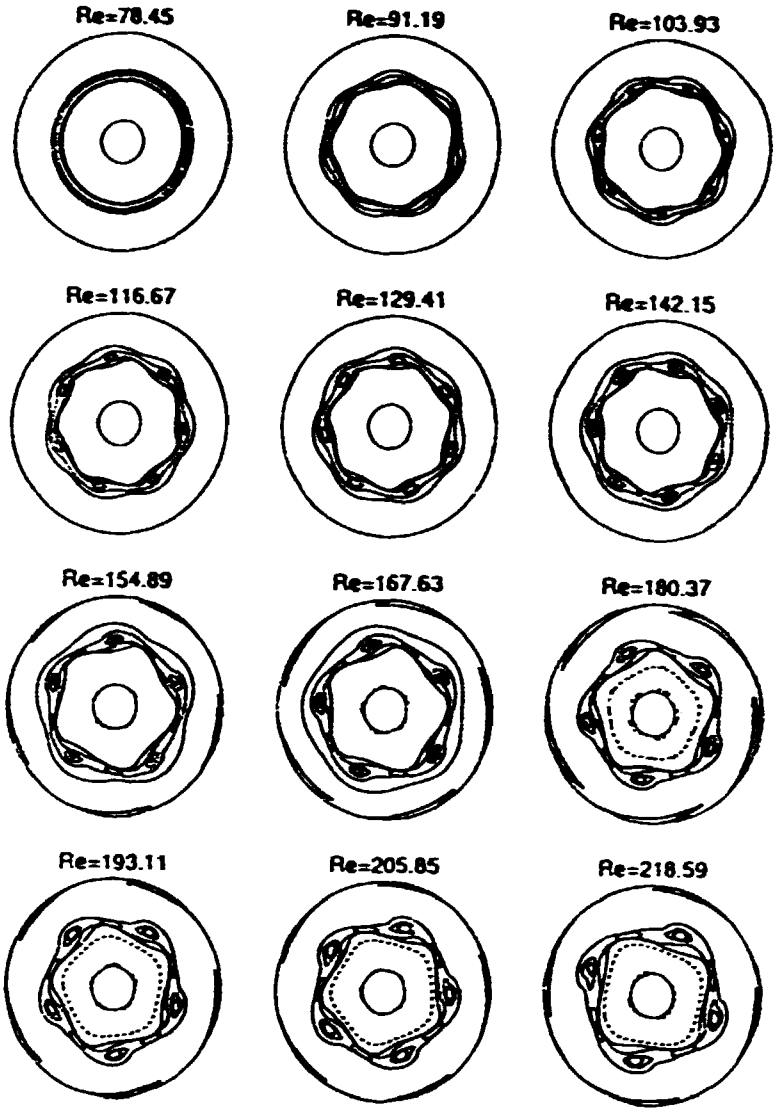


*Figure 1. Numerical simulation of an annular shear layer with slowly increasing forcing. The contour plots show instantaneous vorticity distributions. A small amount of noise was added to the initial, rotationally symmetric, vortice distribution. At the critical Reynolds number, the flow makes a transition to a state with azimuthal mode number m = 7. As the Reynolds number is increased further, the flow undergoes a sequence of symmetry breaking bifurcations to states with lower values of m.*

### 2.1.5 Multidomain Spectral Simulation of Unsteady, Compressible Flow Around a Circular Cylinder

(J.S. Hesthaven, W.S. Dons*, D. Gottlieb* (* Brown University, Division of Applied Mathematics, Providence, RI 02912, USA), and M.D. Salas** (** ICASE, NASA Langley Research Center, Hampton, VA 23665, USA))

The behaviour of compressible flow past a circular cylinder has been used as a

model for fundamental studies of external flows. In spite of the simplicity of the geometry, this simple flow embodies a variety of interesting flow phenomena, ranging from steady Stokes flow to viscous wake flow and fully developed turbulence.

During the last decades the dynamics of unsteady, compressible wake flows past a cylinder have been studied intensively - experimentally as well as theoretically. Recent experiments seem to indicate that coupling to acoustic waves propagating upstream may have a significant impact on the overall dynamics of the flow. These acoustic waves may appear in wind tunnel experiments, where the turbine generates sound waves which propagate downstream, reflect at the end of the wind tunnel and, finally, propagate upstream where they may interfere with the experiment.

In order to study this phenomenon, we have developed a pseudospectral Fourier-Chebychev code, where the computational domain is split into several nonoverlapping subdomains. This allows larger flexibility in choice of grid, grid mappings, and filtering. The artificial outer boundary is treated by employing the method of characteristics for hyperbolic systems of conservation laws, thereby assuming that the flow may be considered inviscid at the outer boundaries. Matching of characteristic waves has also been employed as a patching scheme between the nonoverlapping subdomains. The code can handle flows with Mach number $< 0.6$ and Reynolds number $< 200$, where three-dimensional effects become important.

As an example, in Fig. 1 we see the full computational domain, consisting of three nonoverlapping subdomains used for simulating the flow past a cylinder at $M = 0.4$ and $Re = 108$. In Fig. 1 we also show a contour plot of the relative density $\rho/\rho_\infty$. The formation of the Von-Karman street is clearly demonstrated and the Stroudal number for the shreading is found to be $St = 0.16$, in full accordance with experimental findings. These results clearly demonstrate the applicability of the domain patching and the outer boundary conditions.

The formulation of the scheme as a multidomain approach lends itself to parallel implementation of contemporary parallel coarse-grained architectures. Indeed, we observe a speedup of 1.8 at a two-processor system, illustrating the effectiveness by which such problems may be solved when employing modern computational approaches.

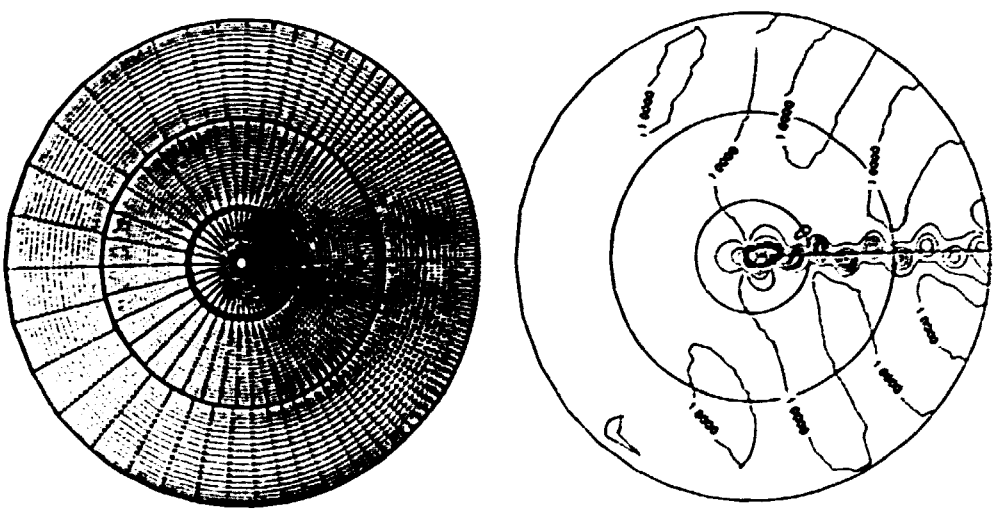

*Figure 1. Computational grid and relative density, $\rho/\rho_\infty$, at $T = 156.21$ for a three-domain simulation of a compressible flow past a cylinder at $M = 0.4$ and $Re = 108$. The Strouhal number, based on the shreading frequency of the vortices and the diameter of the cylinder, is $St = 0.167$.*

In accordance with the experimental findings, we observe that acoustic waves corresponding to a relative pressure perturbation as low as 0.1 % may indeed have a significant impact on the shedding dynamics. However, we also find that heating the cylinder may have an even greater impact on the dynamics. These results are of importance to understanding measurements obtained in wind tunnels by using hot wires.

We plan to conduct a thorough investigation of the effects of the acoustic waves and the heating of the cylinder in order to uncover these new phenomena. We also intend to improve the computer code by employing recent theoretical results which ensure temporal stability of the computational scheme, thus allowing for longtime integration of the governing equations.

### 2.1.6 Linear Stability of a Modon on the $\beta$-Plane

(J.S. Hesthaven, J. Nycander (Uppsala University, Uppsala, Sweden), and J. Juul Rasmussen)

In recent numerical studies it has been shown that modons seem to be linearly unstable, even in parameter regimes where they are known to be nonlinearly stable, i.e. eastward propagating. This counterintuitive result has been obtained for studies of modons in a full spherical geometry. However, due to the complexity of the geometry, the convergence of the growth rate with increased spatial resolution was poor, and one may speculate if the linear instability observed is a numerically induced phenomenon.

In order to study this problem, we have developed a model that allows studies of the linear stability on the $\beta$-plane by using a time integration technique, as opposed to solving the full two-dimensional eigenvalue problem. The simplicity of the $\beta$-plane geometry allows the use of sufficient spatial resolution to gain confidence in the results.

The model is based on a linearisation of the quasi-geostrophic equivalent barotropic equation in a moving reference frame, and an initial perturbation with an energy spectrum $E(k) \sim k^{-3}$ and random phase. As spatial interpolation scheme we used a double periodic spectral scheme and as temporal integration scheme we employed a third order Adam-Bashforth method.

Our study shows good conformity with the results obtained for the full spherical geometry. Although we see slight differences introduced by the differences in geometry, frequency, and growth rate for the most unstable mode, our study clearly confirms the linear instability of the modon.

Careful inspection of results obtained in other studies indicates that the linear instability corresponds to an azimuthal twisting of the structure. This result was also found for the spherical case. However, it is well known that the modon is nonlinearly stable to azimuthal perturbations. This suggests that the linear instability is saturated by nonlinear effects which dominate the dynamics for larger azimuthal perturbations. Indeed, in full nonlinear simulations we observe that for small initial angular perturbations the azimuthal twisting initially grows exponentially, but soon the nonlinear saturation decreases the growth rate to such an extent that the modon, finally, propagates as expected from conservation of potential vorticity

### 2.1.7 Dipole Formation from Breaking Rossby Waves

(G.G. Sutyrin*, I.G. Yushina* (*P.P. Shirshov Institute of Oceanology, Moscow, Russia), J.S. Hesthaven, J.P. Lynov, and J. Juul Rasmussen)

Large-scale quasi-two-dimensional flows in planetary atmospheres and oceans are known to be highly anisotropic due to the variation of the Coriolis parameter with the latitude, the so-called $\beta$-effect, which allows the propagation of Rossby waves. In a magnetised plasma the inhomogeneity of the plasma density gives rise to similar effects and allows the propagation of drift waves. The understanding of the nonlinear dynamics of Rossby waves and drift waves together with the associated transport has important implications on both applied and fundamental atmospheric and oceanic research as well as on fusion research.

Abundant intense vortices in the atmospheres and oceans are capable of generating large amplitude Rossby wave patterns and their interaction with the vortices may strongly affect the general dynamics. A general feature of the evolution of a strong monopolar vortex on the $\beta$-plane is that during the meridional propagation of the vortex it reorganises into a tripolar structure with an elliptical core with vorticity of the same sign as in the original monopole and two satellites with opposite vorticity[1]. Rotation and distortion of the satellites lead to increased mixing near the boundary of the vortex core providing a mechanism for fluid exchange between the vortex core and the generated wave wake field.

Further investigations based on numerical solutions of the quasi-geostrophic equivalent barotropic equation (the so-called Hasegawa-Mima equation in the plasma context) have indicated that there is a critical value for the vortex intensity below which the satellites do not appear. For these intermediate intensities the coupling of the vortex and its wave wake is found to lead to the appearance of large-scale dipole vortices from the breaking of the waves. The dipole will in turn interact with the original monopole vortex leading to increased meridional displacement of the vortex core and providing additional fluid transport. Detailed numerical investigations for a variety of parameters have been conducted to reveal the mechanism of the Rossby wave breaking and the dipole-monopole interaction.

1) Hesthaven, J.S., Lynov, J.P., Rasmussen, J.J., and Sutyrin, G.G. (1993). Phys. Fluids A 5, 1674-1679; Sutyrin, G.G., Hesthaven, J.S., Lynov, J.P., and Rasmussen, J.J. J. Fluid Mech. in press.

### 2.1.8 Dynamics of Nonlinear Dipole Vortices

(J.S. Hesthaven, J.P. Lynov, A.H. Nielsen, J. Juul Rasmussen, M.R. Schmidt* (*University of Odense, Denmark), E.G. Shapiro** and S.K. Turitsyn** (**Institute of Automation and Electrometry, Novosibirsk, Russia))

Stationary solutions to the Euler equations describing two-dimensional flows have a functional relationship between the vorticity, $\omega$, and the stream function, $\psi$, i.e. $\omega = f(\psi)$ ($\omega$ and $\psi$ are related by $\omega = -\nabla^2\psi$). For the simplest case, where $f$ is a linear function one finds, for instance, the so-called Lamb dipole which often appears to be a good approximation to dipoles found in experiments in rotating or stratified fluids. We have numerically found a steadily propagating dipole with a strongly nonlinear relationship between $\omega$ and $\psi$, with $f(\phi) = \alpha\phi + \beta\phi^3 + \gamma\phi^5$ inside a separatrix of almost circular shape and $f(\phi) = 0$ outside the separatrix, "a nonlinear dipole"[1]. Here $\phi$ is the stream function in the frame moving with the dipole. A similar type of dipole has also been found in experiments under certain conditions. We have investigated the nonlinear dynamics of this dipole numerically. In Fig. 1 we show an example of a head-on collision between two nonlinear

dipoles. The two dipoles approach each other, change partners and, finally, two "new" dipoles propagate away in the direction perpendicular to the initial direction of propagation. The two "new" dipoles are identical to the two initial ones. Thus, the dipoles are stable to head-on collisions, as is the Lamb dipole. We have also revealed that an off-axis collision between two nonlinear dipoles may lead to the formation of a tripolar structure, as also found for Lamb dipoles. Making the nonlinear dipole collide head-on with a Lamb dipole, we found that both types of dipoles regenerated after the interaction and continued to propagate along their original direction away from each other.

1) Hesthaven, J.S., Lynov, J.P., Michelsen, P., Nielsen, A.H., Rasmussen, J.J., Schmidt, M.R, Shapiro, E.G. and Turitsyn, S.K. (1993). Risø-R-674, p. 38.

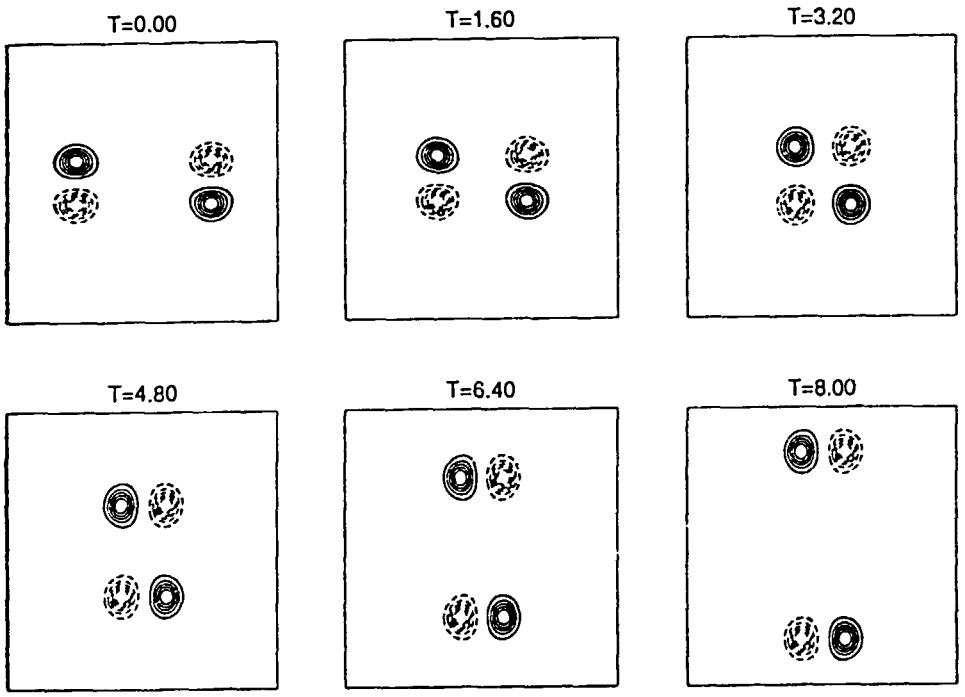


*Figure 1. Contour plots of the vorticity showing the head-on collision of two nonlinear dipoles.*

### 2.1.9 Interaction of Dipolar Vortices with Cylinders

(E.A. Coutsias (University of New Mexico, USA), J.P. Lynov, A.H. Nielsen, J. Juul Rasmussen, and B. Stenum)

The dynamics of dipolar vortices colliding with cylinders are investigated both numerically and experimentally. In the numerical investigations we employ a fully dealiased, spectral scheme based on Fourier-Chebyshev expansions. This allows very high resolution of the boundary layers. The flow field is governed by the two-dimensional Navier–Stokes equation

$$\frac{\partial \omega}{\partial t} + \mathbf{v} \cdot \nabla \omega = \nu \nabla^2 \omega \ .$$

The velocity is given as $\mathbf{v} = \nabla \psi \times \hat{z}$, $\psi$ being the stream function, the vorticity as $\omega = -\nabla^2 \psi$, and $\nu$ is the kinematic viscosity. The flow is subject to no-slip conditions so that it matches the wall velocity at the boundaries. In the numerical studies a Lamb dipole was used as the initial dipolar structure and was made to collide with cylinders of various radii relative to the radius of the dipole.

The results of the numerical investigations were compared with experimental investigations performed in a rotating tank with water (see section 3.2.10). Here the dipolar vortices were generated by injection of dyed jets and made to collide with cylindrical obstacles of different radii. Using the parameters (size and velocity) of the well formed dipoles in the experiment - dipoles which are quite similar to Lamb dipoles - as input to the numerical investigations, we revealed detailed agreement between the numerical and experimental results. The interaction is summarised as follows: as the dipole approaches the cylinder, it induces opposite sign wall vorticity layers. These grow and at a minimum approach the wall layers roll up into tight secondary vortices which couple to the opposing primary lobes. In turn the combined structure detaches from the cylinder thereby splitting the primary dipole into two.

In further numerical investigations we attempted to find a lower limit of the cylinder radius, below which the splitting of the incoming dipole would not occur. For axial collisions we have not found that limit within the possible resolution of the numerical scheme. For a cylinder diameter $D_c$ of 1/64 of the dipole diameter $D_d$, we still observe a splitting as seen in Fig. 1. Note, however, that the original dipole reforms behind the cylinder and propagates away; for larger cylinders it rejoins in front of the cylinder and collides with it again. For off-axis collisions with small cylinders the dipoles were only weakly perturbed and found to reconstruct after the interaction, which agrees with our experimental findings. In addition, from the numerical investigations we observed that the total generated vorticity in the upper half-plan is almost independent of the cylinder radius in the investigated interval ($1/64 \geq D_c/D_d \leq 1$). This is illustrated in Fig. 2, where the time evolution of this generated vorticity is shown for different radii.

In order to further validate our numerical scheme we have initiated a detailed comparison with the results obtained by the group at the University of Rome, Italy[1]. They have made similar investigations by employing a quite different numerical model based on a finite difference scheme. Preliminary comparisons indicate that our spectral scheme is more accurate than the finite difference scheme, in particular for higher Reynolds numbers ($\geq 1000$).

1) Orlandi, P. (1990). Phys. Fluids **A2**, 1429-1436; (1993). Phys. Fluids **A5**, 2196-2206.

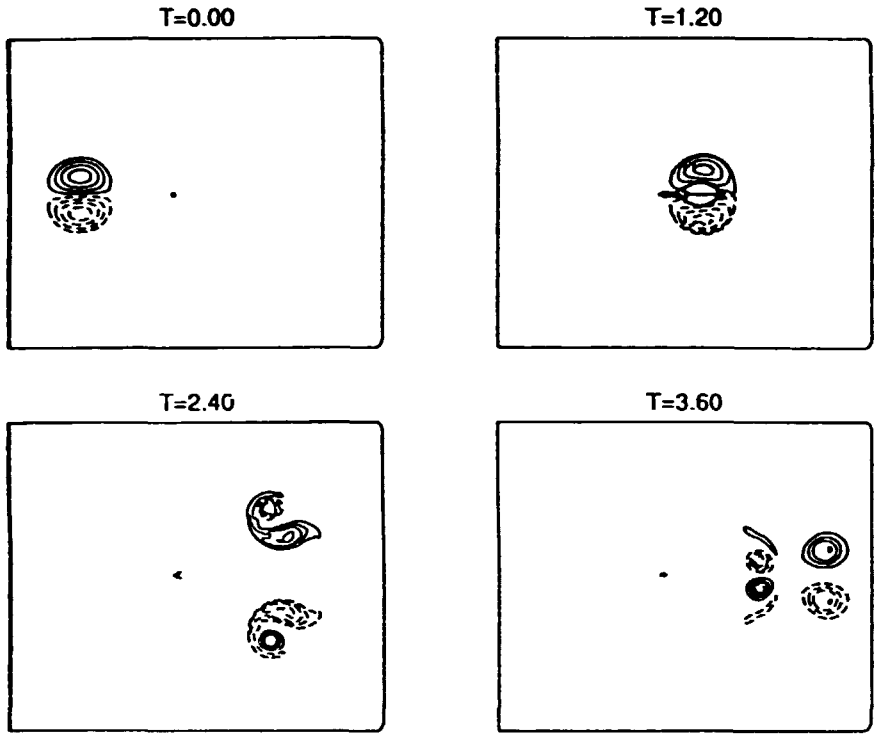


*Figure 1. Interaction of a dipolar vortex with a small cylinder of diameter 1/64 of the dipole diameter.*

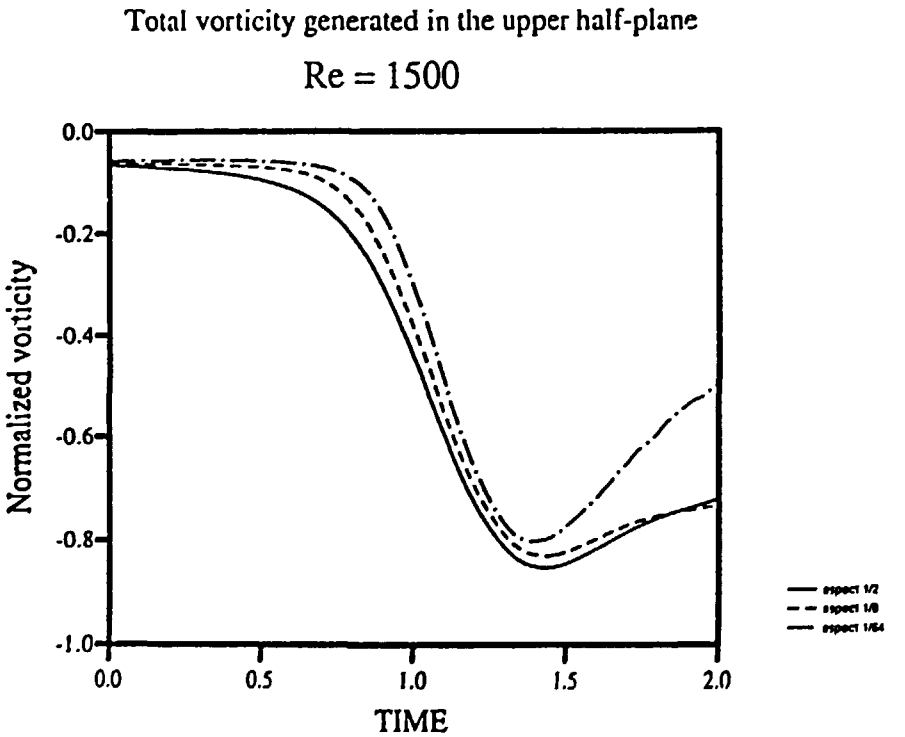


*Figure 2. The time evolution of the total negative vorticity generated during the interaction of the dipole with the cylinder for different values of $D_c/D_d$.*

### 2.1.10 Experimental Investigations of Two-Dimensional Plasma Turbulence

(A.H. Nielsen, M.O. Nielsen, H.L. Pécseli (University of Oslo, Norway), and J. Juul Rasmussen)

The experimental investigations of low frequency, flute-type plasma turbulence were concluded. The investigations were performed in the Q-machine plasma. The Q-machine has now been closed down and dismantled.

The fluctuations were generated by the Kelvin-Helmholtz instability due to a strongly sheared azimuthal flow of the residual plasma surrounding the main plasma column. The radial potential variation in the residual plasma and thereby the azimuthal flow could be controlled by the bias of a limiting aperture inserted perpendicularly to the plasma column. In the last phase of the investigations we concentrated in particular on a detailed analysis of the anomalous plasma transport associated with the turbulence.

In order to monitor the turbulent transport we measured the fluctuations in density, $\tilde{n}$, obtained from the ion saturation current, $j_i$, to a Langmuir probe and the azimuthal electric field component, $\tilde{E}$, obtained from the floating potential difference, $V_{fl}$, measured at two closely spaced Langmuir probes. It should be noted that if there are significant fluctuations in temperature, $\tilde{T}_e$, one cannot directly deduce $\tilde{n}$ and $\tilde{E}$ from $j_i$ and $V_{fl}$, respectively, but has to account for $\tilde{T}_e$. Analysing the resulting radial flux: $\tilde{\Gamma}(t) = \tilde{n}(t)\tilde{E}(t)/B_0$, we obtained detailed information about the plasma transport that can be attributed to the turbulent fluctuations. We interpreted our observation as an indication of the transport in our experiment being a mixture of Brownian type turbulent diffusion and sporadic bursts. By employing a conditional sampling technique to the spatially varying potential and density fluctuations with the flux signal as reference signal, we verified that the bursts in the flux corresponded directly to the presence of coherent vortical structures.

It was explicitly demonstrated that the largest amplitude vortices were actually very effective in transporting plasma, but they occurred so rarely that their accumulated effect was small compared with that of their small amplitude counterparts[1].

The radial dependence of the averaged value of $\tilde{\Gamma}$, $\Gamma_0$, as well as that of the fluctuation levels of both $\tilde{E}$ and $\tilde{n}$ were measured simultaneously for varying conditions. We found that $\Gamma_0$ had the maximum value at a radial position just outside the main plasma column. For larger radii $\Gamma_0$ decreased monotonically almost as $1/r$, where $r$ denotes the radial position. However, the absolute magnitude of $\Gamma_0$ did not appear to be correlated with the absolute fluctuation level and the position of the maximum of $\Gamma_0$ was usually not coinciding with the position of the maximum fluctuation level, as would be expected from considerations based on quasi-linear theory. This is indicated in Fig. 1 where we have plotted the cross-coherence, $\gamma$, defined as:

$$\gamma = \frac{\Gamma_0}{\sqrt{< \tilde{E}^2 >< \tilde{n}^2 >}/B_0}$$

for three different values of the magnetic field. These findings are consistent with the observation that the evolution of the turbulence is dominated by coherent structures. It is, strictly speaking, not meaningful to associate a diffusion coefficient with the transport process described above. However, defining an "effective" diffusion coefficient as $D = \Gamma_0/|\nabla n_0|$ we find that even if there is a clear tendency for $D$ to decrease with increasing $B_0$, our results are not clearly consistent with the Bohm-scaling $D \propto 1/B_0$. Furthermore, we found that the total

turbulent flux, $\Gamma_0$, is consistent with the effective particle flux that can be derived from the density gradient in the residual plasma. Thus, far the dominating transport is fluctuation driven transport. This is also found in the "scrape-off layer" of a Tokamak plasma[2].

In order to assess the importance of possible temperature fluctuations on these measurements we have measured the temperature fluctuations directly in the residual part of the plasma by means of the triple-probe method[3]. We found that the relative level of temperature fluctuations was below 0.1 which is somewhat lower than the relative density fluctuation level and the normalised potential fluctuation level. Furthermore, we found that $\tilde{T}_e$ is almost in phase with $\tilde{n}$ as is seen from the cross-correlation $< \tilde{n}(t)\tilde{T}_e(t+\tau) >$ shown in Fig. 2. This implies that the "error" on our fluxes obtained without correcting for the temperature fluctuations would be below 20%.

1) Huld, T., Nielsen, A.H., Pécseli, H.L., and Rasmussen (1991). J.J., Phys. Fluids B3, 1609-1625; Nielsen, A.H., Pécseli, H.L., and Rasmussen (1992). J.J., Ann. Geophysicae 10, 655-667; Pécseli, H.L., Coutsias, E.A., Huld, T., Lynov, J.P., Nielsen, A.H., and Rasmussen, J.J. (1992). Plasma Physics and Controlled Fusion 34, 2065-2070.

2) Wootton, A.J., Tsui, H.Y.W., and Prager, S. (1992). Plasma Physics and Controlled Fusion 34, 2023-2030.

3) Kamitsuma, M., Chen, S-L., and Chang, J-S. (1977). J. Phys. D: Appl. Phys. 10, 1065-1077.

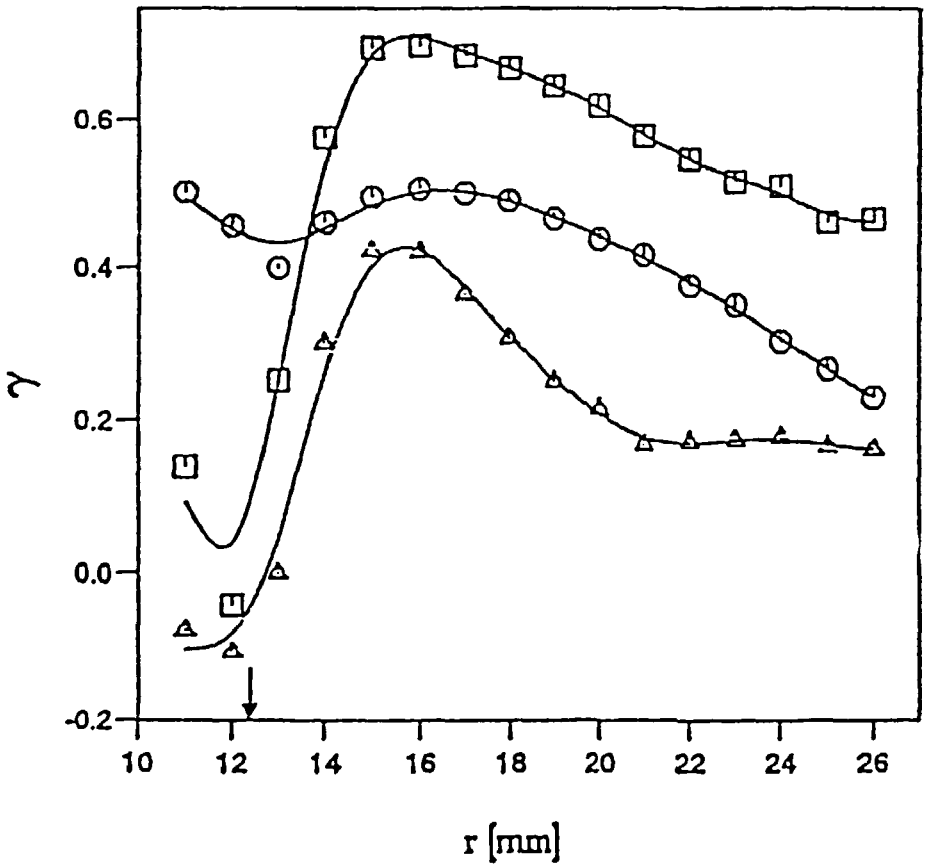


*Figure 1. Radial variation of the cross-coherence $\gamma$ for three different magnetic fields: □ : $B_0 = 0.21\ T$, ○ : $B_0 = 0.28\ T$, and △ : $B_0 = 0.42\ T$. The arrow denotes the edge of the plasma column.*

### 2.1.11 Experimental Evidence for Mode Selection in Turbulent Plasma Transport

(A.H. Nielsen, H.L. Pécseli (University of Oslo, Norway), and J. Juul Rasmussen)

In the experimental investigations of low frequency turbulence in the Q-machine plasma we have obtained evidence for the simultaneous presence of two types of oscillations. One type has the characteristics of drift waves - i.e. the density fluctuations, $\tilde{n}$, are in phase with the potential fluctuations, $\tilde{\phi}$; the relative level, $\tilde{n}/n_0$, is about equal to the normalised potential fluctuation level, $e\tilde{\phi}/T_e$; and the fluctuations propagate with the electron diamagnetic drift velocity. The other type has the characteristics of a flute mode (or convective cell mode) as discussed in section 2.2.1. The two types of modes are distinguished by employing a conditional sampling technique with different conditions applied to the same signal. It is further found that the drift wave type fluctuations do not give any significant contribution to the turbulent transport, while the flute type modes account for the major part of this transport.

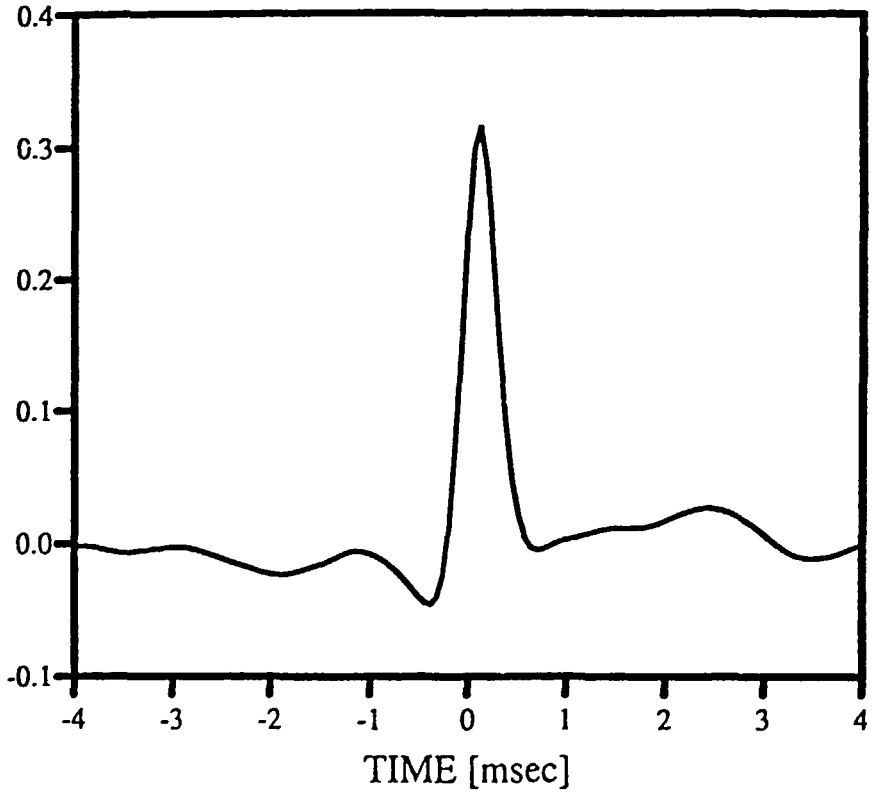


*Figure 1. The cross-correlation* $\langle \tilde{n}(t)\tilde{T}_e(t+\tau)\rangle$.

### 2.1.12 Modulational Instability of Plasma Waves in Two Dimensions

(V.I. Karpman (Racah Institute of Physics, Jerusalem, Israel), J.P. Lynov, P. Michelsen, and J. Juul Rasmussen)

The nonlinear evolution of a two-dimensional modulational instability of plasma waves has earlier been shown either to proceed into an approximate exponential growth of wave amplitude or a recurrent type of behaviour in which wave am-

plitude and density modulation increase and decrease repeatedly. The number of recurrences may depend on initial conditions and on the relevant plasma and wave parameters. In order to understand these processes in more detail we have investigated the evolution by a two-dimensional numerical simulation. As a model we have chosen the equations describing interaction between whistler waves and either fast or slow magnetosonic waves. The equations were solved numerically in a two-dimensional domain with periodical boundary conditions. We employed a fully dealiased spectral method.

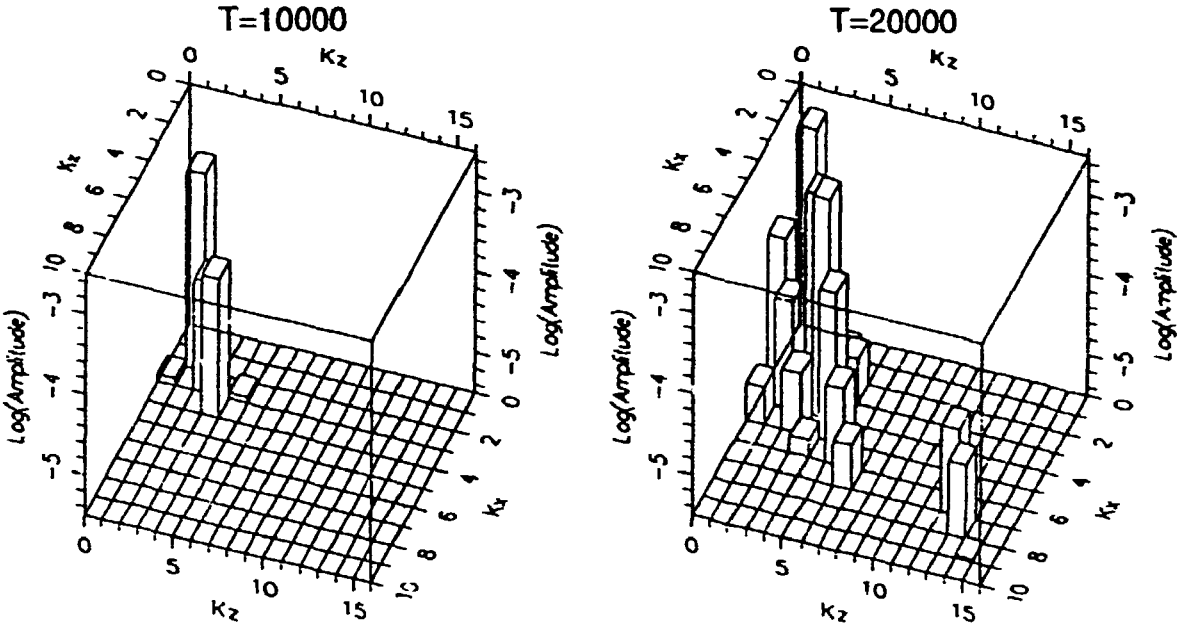


*Figure 1. The mode spectrum for the interaction with the fast magnetosonic mode for two different times. Note the growth of the unstable high order modes.*

The two cases behave differently. For the case of the interaction with the fast wave, the instability is in general found to evolve in a quasi-recurrent manner in which the main part of the energy resides in the fundamental mode of the initial modulation. For the longtime evolution the energy is spreading slowly to larger and larger wave numbers resulting in a random wave field. As the initial condition the whistler wave is modulated almost perpendicularly to its direction of propagation along the z-axis, i.e. the ratio of the modulational wave numbers. $\alpha = K_z/K_x \ll 1$. This corresponds to the region of modulational instability with the maximum growth rate obtained for a certain $\alpha_c$. For low amplitudes and $\alpha = \alpha_c$ the evolution shows three clear recurrence periods before the spreading of the energy becomes significant. This behaviour is well described by a simplified model based on a generalised Hamiltonian and truncated to involve only few modes. For increasing wave amplitude the recurrent feature becomes less pronounced and the spreading of the energy to higher modes proceeds faster. For a given amplitude the evolution is found to depend strongly on the value of $\alpha$, having a maximum of recurrence for $\alpha$ close to $\alpha_c$. For $\alpha > \alpha_c$ the recurrence first becomes a little better and then worse. However, in this region it is interesting to note that it is important to include a large number of modes ($64 \times 64$ at least) to get the correct result. With fewer modes several additional recurrences show up. For $\alpha < \alpha_c$ the spreading to the higher modes proceeds considerably faster: already for $\alpha = 0.99\ \alpha_c$ only one recurrence period is observed. The observed fea-

tures may be qualitatively explained from knowledge of the dispersion relation and growth rate of the linear waves. In Fig. 1 an example of the evolution of the mode spectrum is shown. Note the growth of the unstable higher order modes which are nonlinearly excited. These modes will in turn dominate the evolution and it is clear that the asymptotic development would be significantly altered if the system was truncated and these modes not included. For the case of interaction between whistler waves and the slow magnetostatic waves a clear recurrent behaviour was not observed, and the energy was constantly spreading to the higher mode numbers, which is in agreement with predictions of a qualitative analytical theory. The modulation has a spatial structure resembling cells stretched along the z-axis.

### 2.1.13 Plasma Transport Due to Electrostatic Turbulence

(Bo Gervang, J.P. Lynov, P. Michelsen, and J. Juul Rasmussen)

The energy confinement of a fusion plasma is limited by the radial heat and particle transport. This transport has long been known to be much larger than the one calculated from the classical theory of diffusion. The so-called anomalous diffusion is believed to be due to electrostatic and magnetostatic fluctuations of micro-instabilities in the plasma driven by density and temperature gradients which cause an enhanced radial plasma transport. Fluid simulations oriented to understand this transport have resulted in transport coefficients in agreement with those found analytically from quasi-linear theory. However, the results can only in some cases describe the experimental results correctly, but cannot at all describe some phenomena such as the transition between the low and high confinement (L- and H-mode).

A theoretical and numerical study was initiated in order to investigate specific physical phenomena of the transport, especially those connected with transport due to coherent structures. This study is concentrated on electrostatic modes in magnetised plasmas, such as drift waves and $\eta i$ modes, and also includes the effect of velocity shear which may be important for the transition from L- to H-modes in tokamak plasmas. The numerical methods are based on the highly accurate spectral methods that have been developed in the section mainly for investigations of fluid dynamic systems in which large-scale coherent structures are a typical feature of two-dimensional turbulence. It is not clear whether such structures will exist in more complex models where two or more fields are coupled. However, it has been shown that they may exist in simplified models for the $\eta i$ modes. If they also appear under more realistic conditions, they will have strong influence on the modelling of transport. Scaling arguments based on quasi-linear transport coefficients will consequently not be adequate.

### 2.1.14 Visualisation of Numerical Data

(L. Bækmark, J.P. Lynov, and P. Michelsen)

The visualisation program FRAME described last year was further developed and implemented on the new HP-735 workstation. The purpose of the program, which is based on the UNIRAS graphical system, is to make the data visualisation process easy and flexible for the user. The program is made for visualisation of a time sequence of two-dimensional flow data, but can be used for all kinds of 2D or 3D data sets. A collection of transformation subroutines was developed to provide the possibility of transforming the input data before the visual presentation. The input flow data may be, e.g., Fourier or Chebyshev modes, and can, after the

relevant inverse transformation, be presented in configuration space. The screen and hardcopy presentation consist of a number of plots (contour, surface, etc.) each placed in a spreadsheet system of rows and columns. After transformations and processing new data files may be produced: (a) unipict files for further processing and layout adjustments with the UNIEDIT program, (b) targa files for video animation of longtime sequences or for dias production, and (c) HDF-files to be used with the NCSA Ximage/Collage program for direct animation on screen. Examples of output may be found in other contributions of this report.

### 2.1.15 A Phase Screen Approach to Coherent Scattering in Fluids

(R.V. Edwards (Case Western Reserve University, Cleveland, Ohio, USA), L. Lading, and V.O. Jensen)

Laser anemometry (velocimetry) based on particle scattering is well established. However, in certain fluids particles cannot be present. This is, e.g., the case in a fusion plasma. In such systems it may be possible to measure transport properties of large-scale fluctuations on the basis of light scattering/diffraction from small-scale structures convected by the larger scales[1]. We have adapted a phase screen approach to the analysis of such systems. A two-point correlation scheme has been devised that allows for a better spatial selectivity than conventional reference beam Doppler systems. The concept is based on a combination of time-of-flight and Doppler systems with reference beam detection. The principle may make it possible to separate different types of waves that generate turbulence.

1) Truck, A. et al. (1992). "ALTAIR": An infrared laser diagnostic on the TORE SUPRA Tokamak", Rev. Sci. Instrum. 63, 3716-3724.

### 2.1.16 Magnetic Stresses in Ideal MHD Plasmas

(V.O. Jensen)

A comprehensive study of the advantages of using magnetic stresses for determining steady state equilibria of ideal MHD plasmas has been undertaken. The basic equations are:

$$\text{the force density equation,} \quad \mathbf{j} \times \mathbf{B} = \nabla p, \tag{1}$$

$$\text{the Maxwell equations,} \quad \nabla \times \mathbf{B} = \mu \mathbf{j} \quad \text{and} \quad \nabla \cdot \mathbf{B} = 0. \tag{2}$$

Although the magnetic force densities given by the left-hand side term in Eq. (1) are volume forces, it appears that the resulting force on any finite volume element in a plasma can always be calculated by integrating magnetic stresses and particle pressures over the surface of the element. Equilibrium then requires the resulting forces to vanish. Expressions are derived for the various stresses that transmit forces through a surface element, see Fig. 1. Clearly, it is advantageous to choose, whenever possible, volumes with surfaces that are either parallel or perpendicular to the magnetic lines of force. For such surfaces the magnetic stresses are reduced to an isotropic compressive stress, $B^2/2\mu_o$, and a tensile stress, $B^2/\mu_o$, acting parallel to the field lines.

The main purpose of this study is to demonstrate that magnetic stresses offer an alternative and simple method to calculate equilibrium conditions for ideal MHD plasmas. The method has the advantage of offering a simple, physical interpretation of the various terms encountered in the calculations. It also facilitates an assessment of the approximations used in the derivations. Finally, the improved physical understanding facilitates a quick assessment of the impact on the plasma of imposed changes in the confining field.

**In this work conditions for equilibria of axisymmetric toroidal plasmas are reconsidered. It is shown that a purely toroidal magnetic field can prevent a plasma from expanding in the direction of the minor radius only at the expense of an expansion in the direction of the major radius which is twice as fast as it would have been without the toroidal field. The virial theorem is rederived and discussed in terms of the magnetic stresses. Finally, the Grad-Shafranov shift is rederived, and all the terms in the expression for the shift are explained in terms of magnetic stresses.**

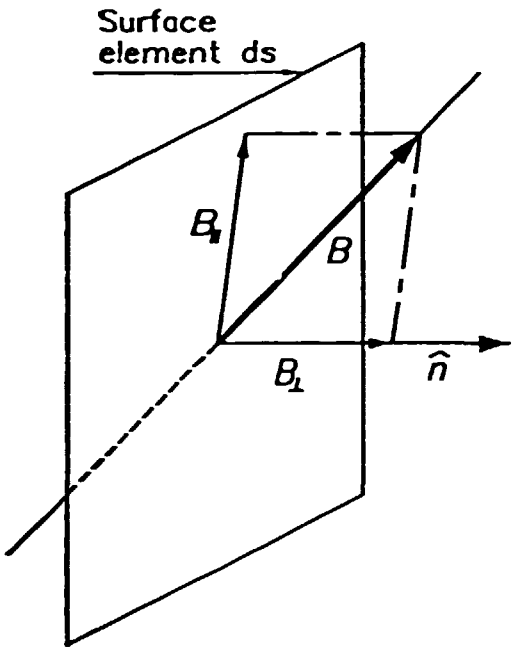


Active stresses

| | | |
|---|---|---|
| Shear : | $B_\parallel B_\perp/\mu_o$ | $[\uparrow(\hat{B}_\perp \times \hat{B}_\parallel) \times \hat{n}]$ |
| Tensile : | $B_\perp^2/\mu_o$ | $[\longrightarrow \hat{n}]$ |
| Compressive : | $B^2/2\mu_o$ | $[\longleftarrow -\hat{n}]$ |
| Particle pressure : | $p$ | $[\longleftarrow -\hat{n}]$ |

***Figure 1. Active stresses acting on a surface element ds. n is a unit vector normal to ds. The forces are transmitted through ds to the volume behind ds. The directions of the various forces are indicated in the brackets with arrows and given in vector expressions.***

## 2.2 Pellet Handling, Acceleration, and Injection

### 2.2.1 Construction of Multishot Pellet Injectors for FTU, Frascati, and RFX, Padova

**(H. Sørensen, A. Michelsen, B. Sass, K-V. Weisberg, and J. Bundgaard* (*Engineering and Computer Department))**

The multishot pellet injector systems developed at Risø have the following main characteristics:

- Eight pellets units.
- Pneumatic acceleration, fast valve, high pressure reservoir.

- In situ pellet condensation.
- Velocities ~500 to ~1500 m/s.
- $D_2$ and $H_2$ pellets, $5 \cdot 10^{18}$ to $4 \cdot 10^{20}$ atoms/pellet.
- Mass and velocity measured in flight.
- High reproducibility:
  - mass ±10%,
  - velocity ±3%,
  - angle scatter ~ 0.025°.
- Minimum driver gas into the plasma.
- Low liquid He consumption (~ $4\ell/h$).

During the period from the spring of 1992 to the end of 1993 a multishot pellet injector for FTU was built, tested, and delivered to Frascati in December 1993.

During the construction improvements were made and various unexpected problems were met and solved:

- A state machine control is installed as an improvement relative to the earlier used automatic operation which was based on a simple PLC.
- The injector system can fire two pellet sizes $H_2$ and $D_2$: six pellets with $1 \cdot 10^{20}$ atoms/pellet and two pellets with $2 \cdot 10^{20}$ atoms/pellet. Unexpected problems in obtaining these pellet sizes were solved.
- Finally, the uplining of the gun barrels caused unexpected problems partly due to contamination of pellet gas. Some of the contamination problems were solved by changing operation procedures. An improved alignment system for the barrels was introduced. These problems caused a delay of nearly four months of the acceptance test.

Parallel with the work on the FTU injector nearly all parts for the RFX injector have been procured and the assembling of this injector was started in December 1993. The injector is scheduled to be delivered in Padova in May 1994.

## 2.3 Work for JET

### 2.3.1 Experimental Investigation of Edge Localised Modes in JET

(A. Lindholm Colton)

Tokamak plasmas are known to exist in two different modes: an *L*-mode with low confinement and an *H*-mode with high confinement. When in an *H*-mode it is known that edge localised modes (ELMs) can occur on the surface of the plasma. These ELMs tend to increase the particle losses from the plasma. In general, ELMs should therefore be avoided, but controlling their appearance might give the possibility of controlling the plasma density.

The aim of the investigation was to examine the nature of ELMs occurring in the JET plasma with the purpose of finding ways to predict and control their appearance. The main findings during the work are:

- The development of temperature and density profiles in an *H*-mode plasma is studied.
- The changes in temperature and density profiles during ELMs are measured.
- The level of fluctuations during ELMs is measured.

- The repetition frequency of the occurrence of ELMs in a newly formed *H*-mode plasma is determined.
- Characteristic orbits in a temperature-density plot during ELMs are found (see Fig. 1).

The main conclusion from the work is that it is very likely that it will be possible to find ways to control and master the occurrence of ELMs in the JET plasma to such a degree that they can be used as a tool for controlling the profile of the plasma density and temperature and thereby keep the plasma in the *H*-mode for a long time. Much more exploratory work has, however, to be carried through to reach that goal.

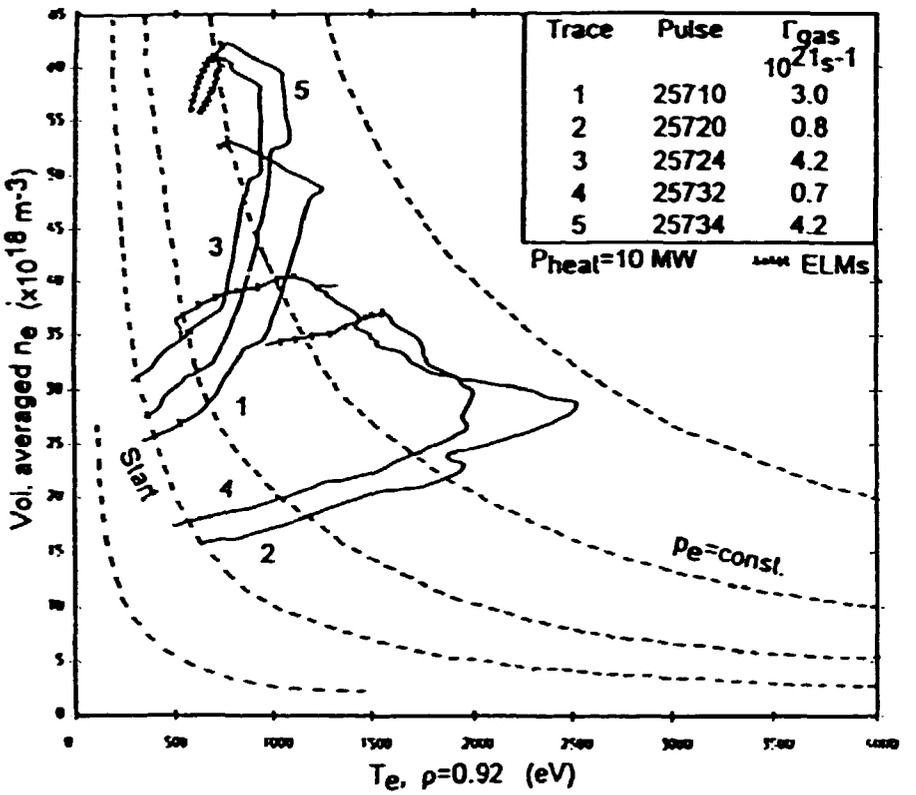


*Figure 1. The trajectory in n-T space during the H-mode and the ELMs period afterwards for five discharges with varying gas fuelling rate and similar heating power.*

## 2.4 Participants in the Work in Plasma and Continuum Physics

**Scientific Staff**
Gervang, Bo (from 1 October)
Grimley, Hugh (from 25 January to 31 December)
Jensen, Vagn O.
Lading, Lars
Lynov, Jens-Peter
Michelsen, Poul
Nielsen, Anders H.
Rasmussen, Jens Juul
Stenum, Bjarne
Sørensen, Hans
Weisberg, Knud-V.

**Ph.D. Students**
Andersen, Annette (until 31 July)
Hesthaven, Jan S.

**Technical Staff**
Astradsson, Lone
Bækmark, Lars
Michelsen, Agnete
Nielsen, Mogens O.
Reher, Børge
Thorsen, Jess

**Secretaries**
Jensen, Elin (from 15 December)
Skaarup, Bitten
Toubro, Lene

**Guest Scientist**
Bergeron, K., University of New Mexico, USA
Edwards, R.V., Case Western Reserve University, Cleveland, USA
Karpmann, V.I., Racah Institute of Physics, Jerusalem, Israel
Kuznetsov, E.A., Landau Institute for Theoretical Physics, Moscow, Russia
Pécseli, H.L., University of Oslo, Norway

**Short-Time Visitors**
Coutsias, E.A., University of New Mexico, USA
Grésillon, D., Laboratoire de Physique des Milieux Ionisés du CNRS, Ecole Polytechnique, Palaiseau, France
Nycander, J., University of Uppsala, Sweden
Turitsyn, S.K., Institute of Automation and Electrometry, Novosibirsk, Russia

**Student Assistants**
Poul Erik Bak (1 October - 30 November)
Schmidt, Michel (18-29 January, 9 August - 17 September, 16-23 December)

## 2.5 Publications and Educational Activities

### 2.5.1 Publications


Bang, O.; Rasmussen, J. Juul; Christianser., P.L., On localization in the discrete nonlinear Schrödinger equation. Physica D (1993) v. 68 p. 169-173.

Bergeron, K.; Coutsias, E.A.; Lynov, J.P.; Nielsen, A.H., Numerical simulations of self-organization in 2-D circular shear flows. In: Dynamics and geometry of vortical structures. EUROMECH 305. ERCOFTAC workshop, Cortona (IT), 28 June - 2 July 1993. (Universita Degli Studi Di Roma La Sapienza, Rome, 1993) p. 118-119.

Coutsias, E.A.; Lynov, J.P.; Nielsen, A.H.; Nielsen, M.; Rasmussen, J. Juul; Stenum, B., Numerical and experimental investigations of dipole interactions with straight and curved walls in 2D flows. In: Dynamics and geometry of vortical structures. EUROMECH 305. ERCOFTAC workshop, Cortona (IT), 28 June - 2 July 1993. (Universita Degli Studi Di Roma La Sapienza, Rome, 1993) p. 116-117.

Coutsias, E.A.; Lynov, J.P.; Nielsen, A.H.; Nielsen, M.; Rasmussen, J. Juul; Stenum, B., Two dimensional flow simulations. In: Proceedings of the European convex users conference. The metacomputing concept: Supercomputing power without boundaries. ECUC 93, Bilbao (ES), 27-29 October 1993. (Centro Vasco de Supercomputacion, Zamudio, Bizkaia, 1993) 4 p.

Coutsias, E.A.; Lynov, J.P.; Nielsen, A.H.; Nielsen, M.; Rasmussen, J. Juul; Stenum, B., Vortex dipoles colliding with curved walls. In: Future directions of nonlinear dynamics in physical and biological systems. NATO Advanced Study Institute on future directions of nonlinear dynamics in physical and biological systems, Lyngby (DK), 23 July - 1 August 1992. Christiansen, P.L.; Eilbeck, J.C.; Parmentier, R.D. (eds.), (Plenum Press, New York, 1993) (NATO Advanced Science Institutes Series B: Physics, 312) p. 51-54.

Ellegaard, O.; Schou, J.; Sørensen, H.; Pedrys, R.; Warczak, B., Sputtering of solid nitrogen by keV helium ions. Nucl. Instrum. Methods Phys. Res. B (1993) v. 78 p. 192-197.

Hesthaven, J.S.; Lynov, J.P.; Nycander, J., Dynamics of nonstationary dipole vortices. Phys. Fluids A (1993) v. 5 p. 622-629.

Hesthaven, J.S.; Lynov, J.P.; Rasmussen, J. Juul; Sutyrin, G.G., Transport properties of isolated vortices on the beta-plane. In: Dynamics and geometry of vortical structures. EUROMECH 305. ERCOFTAC workshop, Cortona (IT), 28 June - 2 July 1993. (Universita Degli Studi Di Roma La Sapienza, Rome, 1993) p. 120-121.

Hesthaven, J.S.; Lynov, J.P.; Rasmussen, J. Juul; Sutyrin, G.G., Vortex dynamics in 2-dimensional flows. In: Future directions of nonlinear dynamics in physical and biological systems. NATO Advanced Study Institute on future directions of nonlinear dynamics in physical and biological systems, Lyngby (DK), 23 July - 1 August 1992. Christiansen, P.L.; Eilbeck, J.C.; Parmentier, R.D. (eds.), (Plenum Press, New York, 1993) (NATO Advanced Science Institutes Series B: Physics, 312) p. 59-62.

Hesthaven, J.S.; Lynov, J.P.; Rasmussen, J. Juul; Sutyrin, G.G., Generation of tripolar vortical structures on the beta plane. Phys. Fluids A (1993) v. 5 p. 1674-1678.

Huld, T.; Nielsen, A.H.; Pécseli, H.L.; Rasmussen, J. Juul, Experimental investigations of two-dimensional plasma turbulence. In: Current research on fusion, laboratory and astrophysical plasmas. International workshop on plasma physics, Pichl (AT), 28 February - 2 March 1991. Kuhn, S.; Schöpf, K.; Schrittwieser, R. (eds.), (World Scientific, Singapore, 1993) p. 243-261.

Karpman, V.I., Radiation by solitons due to higher-order dispersion. Phys. Rev.

E (1993) v. 47, p. 2073-2082.

Lindholm Colton, A., Experimental investigation of edge localised modes in JET. Risø-R-700(EN) (1993) 164 p.

Lynov, J.P.; Rasmussen, J. Juul, Turbulens og selvorganisering i to-dimensionale systemer. KVANT, Fysisk Tidsskrift (1993), v. 4, No. 4, p. 24-28.

Nielsen, A.H., Electrostatic turbulence in strongly magnetized plasmas. Risø-R-659(EN) (1993) 81 p.

Nycander, J., The difference between monopole vortices in planetary flows and laboratory experiments. J. Fluid Mech. (1993), v. 254, p. 561-577.

Nycander, J.; Lynov, J.P.; Rasmussen, J. Juul, Monopolar vortices in etai-modes. Europhys. Lett. (1993) v. 23 p. 249-255.

Lading, L.; Lynov, J.P.; Skaarup, B. (eds.), Optics and Fluid Dynamics Department. Annual progress report for 1992. Risø-R-674(EN) (1993) 58 p.

Stenum, B.; Schou, J.; Sørensen, H.; Gürtler, P., Luminescence from pure and doped solid deuterium irradiated by keV electrons. J. Chem. Phys. (1993) v. 98 p. 126-134.

Sørensen, H.; Sass, B.; Weisberg, K.-V.; Oomens, A.A.M.; Dijk, G. van; Tielemans, A.J.H., A multishot pellet injector for RTP. In: Fusion technology 1992. Vol. 1. 17. Symposium on fusion technology, Rome (IT), 14 - 18 September 1992. Ferro, C.; Gasparotto, M.; Knoepfel, H. (eds.), (Elsevier Science Publishers, Amsterdam, 1993) p. 647-650.

### 2.5.2 Unpublished Contributions

Coutsias, E.A.; Lynov, J.P.; Nielsen, A.H.; Rasmussen, J. Juul; Stenum, B., Experimental investigations of dipole interactions with straight and curved walls in 2-D flows. In: Interaction between vorticity fields and boundaries. Book of abstracts. EUROMECH colloquium 300, Istanbul (TR), 27-30 September 1993. Kaykayoglu, C.R.; Graham, J.M.R. (eds.), (European Mechanics Council, Istanbul, 1993) p. 23.

Coutsias, E.A.; Lynov, J.P.; Nielsen, A.H.; Rasmussen, J. Juul; Stenum, B., Numerical investigations of dipole interactions with straight and curved walls in 2-D flows. In: Interaction between vorticity fields and boundaries. Book of abstracts. EUROMECH colloquium 300, Istanbul (TR), 27-30 September 1993. Kaykayoglu, C.R.; Graham, J.M.R. (eds.), (European Mechanics Council, Istanbul, 1993) p. 24.

Hesthaven, J.S., Transport properties of isotropic and anisotropic flows illustrated by particle dynamics. Paper P24. In: Danish Physical Society spring meeting. Abstracts. Danish Physical Society spring meeting, Rødby (DK), 16-18 May 1993. (Danish Physical Society. H.C. Ørsted Institute, Copenhagen, 1993) p. 48.

Jensen, V.O., Plasmafysik 2. Forelæsningsserie. Danmarks Tekniske Højskole, Lyngby (DK), February - June 1993. Unpublished.

Jensen, V.O., Drømmen om en ubegrænset energi. Danmarks Radio TV, Copenhagen (DK), 4 April 1993. Unpublished.

Jensen, V.O., Status of the European fusion programme: JET, ITER. Paper D4. In: Danish Physical Society spring meeting. Abstracts. Danish Physical Society spring meeting, Rødby (DK), 16-18 May 1993. (Danish Physical Society. H.C. Ørsted Institute, Copenhagen, 1993) p. 17.

Jensen, V.O., Compressive and tensile stresses in magnetic fields used as a basis for calculations of plasma equilibria. Paper P25. In: Danish Physical Society spring meeting. Abstracts. Danish Physical Society spring meeting, Rødby (DK), 16-18 May 1993. (Danish Physical Society. H.C. Ørsted Institute, Copenhagen, 1993) p. 49.

Jensen, V.O., Risø, year 2000, a strategy. In: Physics problems of ITER and DEMO and possible contributions from existing devices and agreed upgrades and programmes. Workshop on physics problems of ITER and DEMO and possible contributions from existing devices and agreed upgrades and programmes, Lisbon (PT), 24-25 July 1993. (Instituto Superior Técnico, Lisbon, 1993) p. 171-180.

Jensen, V.O., Fusionsforskningen har passeret en milepæl. Elsam, Fredericia (DK), 6 May 1993. Unpublished. Abstract available.

Jensen, V.O., Fusionsinterview i serien "Strejftog i Universet", Danmarks Radio, TV, Copenhagen (DK), 20 September 1993. Unpublished.

Jensen, V.O., Fusionsplasmafysik. Forelæsningsserie. Danmarks Tekniske Højskole, Lyngby (DK), September - December 1993. Unpublished.

Lynov, J.P., Coherent structures in two-dimensional flows. Paper M2. In: Danish Physical Society spring meeting. Abstracts. Danish Physical Society spring meeting, Rødby (DK), 16-18 May 1993. (Danish Physical Society. H.C. Ørsted Institute, Copenhagen, 1993) p. 31.

Michelsen, P.; Karpman, V.I.; Lynov, J.P.; Rasmussen, J. Juul, Modulational instability due to nonlinear coupling between high- and low-frequency waves. 5. European fusion theory conference, Madrid (ES), 22-24 September 1993. Unpublished. Abstract available.

Nielsen, A.H.; Bergeron, K.; Coutsias, E.A.; Lynov, J.P., Numerical simulations of self-organization in 2-d circular shear flows. Paper P23. In: Danish Physical Society spring meeting. Abstracts. Danish Physical Society spring meeting, Rødby (DK), 16-18 May 1993. (Danish Physical Society. H.C. Ørsted Institute, Copenhagen, 1993) p. 48.

Rasmussen, J. Juul, Vortex dynamics in two-dimensional flows. 28. Nordic plasma and gas discharge symposium, Wadahl (NO), 8-10 February 1992. Unpublished.

Rasmussen, J. Juul, Vortex dynamics in fluids and plasmas. Physikalisches Kolloquium. Universität Kiel, Kiel (DE), 22 June 1993. Unpublished.

Rasmussen, J. Juul, Two dimensional plasma turbulence. Institut für Experimentalphysik. Universität Kiel, Kiel (DE), 23 June 1993. Unpublished.

Rasmussen, J. Juul, Kohærente strukturer i kontinuumsystemer. Institutkollokvium. Fysisk Institut. Odense Universitet, Odense (DK), 12 October 1993. Unpublished. Abstract available.

Rasmussen, J. Juul, Electrostatic waves and instability in homogeneous, magnetized plasmas. (5 Lectures). Advanced school on waves and instabilities in plasmas. International Centre for Mechanical Sciences, Udine (IT), 20-24 September 1993. Unpublished.

Rasmussen, J. Juul; Stenum, B., Visualization of coherent structures. Optical diagnostics for flow processes. Summerschool, Risø (DK), 26 September - 2 October 1993. Unpublished.

Rasmussen, J. Juul; Stenum, B., Vortices and self-organization in two-dimensional flows. Department of Technical Physics. University of Eindhoven, Eindhoven (NL), 7 December 1993. Unpublished.

Rasmussen, J. Juul; Stenum, B., Eksperimentelle undersøgelser af hvirvelstruktur i væsker. Folkeuniversitetet i Roskilde, Risø (DK), 1 December 1993. Unpublished. Abstract available.

# 3 Work in Fusion Technology

## 3.1 Irradiation Effects

### 3.1.1 Differences in Damage Accumulation in Copper Irradiated with 2.5 MeV Electrons and Fission Neutrons

(B.N. Singh, M. Eldrup, A. Horsewell, P. Ehrhart and F Dworschak (Forschungszentrum Jülich, Germany))

Over the years, a large number of experiments have been carried out to "simulate" the damage accumulation that might occur in the environment of fusion neutrons. In the absence of an intense source of fusion neutrons, these experiments have been carried out using a variety of projectile particles with energies varying in a very wide range. Furthermore, for practical reasons, most of these experiments have been carried out at much higher damage rates than that expected in a fusion reactor. As a result, the effect of recoil energy on damage accumulation still remains poorly known and understood. The present experiments were designed, first of all, to determine the effect of recoil energy on damage accumulation. Another objective of these experiments was to verify one of the major predictions of the newly proposed "production bias" model for defect accumulation under cascade damage conditions. The model predicts, for example, that the damage accumulation under cascade damage (e.g. under fission and fusion neutron irradiation) conditions would be substantially different from that under the conditions of single displacement production (e.g. 1 MeV electrons and low energy light-ions) particularly at low doses.

To meet these objectives, specimens of pure copper were irradiated with 2.5 MeV electrons (at Jülich) and fission neutrons (at Risø) at 523K. These projectiles were chosen because they produce recoil of very different energies and displacement damage in very different forms: single vacancies and SIAs (self-interstitial atoms) are produced by 2.5 MeV electrons whereas fission neutron produce multi-displacement cascades and subcascades. Both sets of experiments were carried out with a similar damage rate (of the order of $\sim 10^{-8}$ NRT dpa/s). Post)irradiation defect microstructures were investigated using electrical resistivity, transmission electron microscopy (TEM) and positron annihilation technique (PAT).

Microstructural investigations showed that the accumulation of defects in the form of planar clusters as well as voids was entirely different in the electron and neutron irradiated specimens (Table 1). Practically no defect clusters were observed in the specimen electron irradiated to a dose level of $\sim$ 0.01 dpa. The specimen irradiated with fission neutrons to the same dose level and at the same temperature (523 K) showed a cluster density of $\sim 10^{22}$ $m^{-3}$. The void density in the electron irradiated copper ($\sim$ 0.01 dpa, 523 K) was found to be more than two orders of magnitude lower than that in the neutron irradiated specimen. Swelling results for the two cases are shown in Fig. 1. It can be easily seen that the swelling in the electron irradiated specimen is about 30 times lower than that in the neutron irradiated specimen. The result of positron annihilation investigations are consistent with the TEM results. The lifetime spectra for the electron and neutron irradiated specimens (both irradiated to $\sim$ 0.01 dpa) are shown in Fig.2. Both spectra contain a short-lived and at least one long-lived component, the latter arising from positrons trapped in defects.

**Table 1: Irradiation-induced microstructural parameters in OFHC-copper irradiated with 2.5 MeV electrons and fission neutrons at ~ 523 K.**

| Projectile particle | Dose (dpa) | Cluster density ($m^{-3}$) | Void density ($m^{-3}$) | Void diameter (nm) | Void swelling (%) |
|---|---|---|---|---|---|
| 2.5 MeV electrons | 0.0023<br>0.013 | -<br>- | -<br>$0.2\text{-}1.2\times10^{19}$ | -<br>13.8 | -<br>$0.2\text{-}1\times10^{-3}$ |
| Fission Neutrons | ~0.001<br>~0.01<br>~0.1<br>~0.3 | $1 \cdot 1 \times 10^{22}$<br>$2 \cdot 9 \times 10^{22}$<br>$5.5 \times 10^{22}$<br>$6.8 \times 10^{22}$ | $6.1 \times 10^{20}$<br>$1.1 \times 10^{21}$<br>$4.2 \times 10^{20}$<br>$6.1 \times 10^{20}$ | 4.5<br>7.7<br>14.6<br>16.1 | 0.002<br>0.02<br>0.06<br>0.13 |

Clearly, the intensity of this defect part of the spectrum for the neutron irradiated specimen is considerably higher than that for the electron irradiated specimen. More quantitative analysis of the lifetime data lead to the same conclusion.

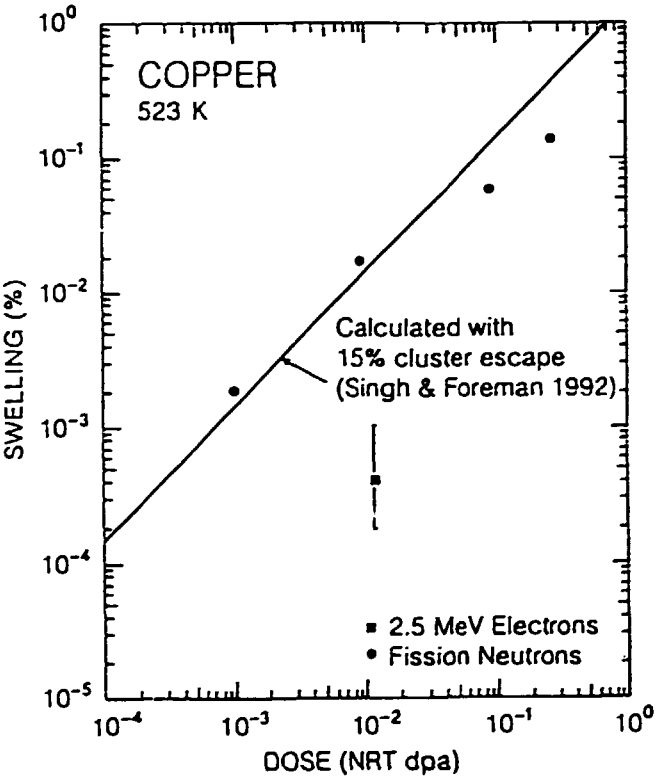


*Figure 1. Dose dependence of void swelling in copper irradiated with electrons and neutrons at 523 K. For comparrison, results on void swelling calculated in terms of production bias model (Singh and Foreman, 1992) are also shown (solid line).*

It has been argued that the difference in the damage accumulation behaviour between electron and neutron irradiations originates from the fundamental difference in the form in which displacements are produced during electron (single defects) and neutron (cascades) irradiations. The intracascade clustering of SIAs and vacancies is the basic cause of the higher defect accumulation rate observed

in the case of neutron irradiation. Since these experiments were carried out on the same material, with the same initial microstructure and under almost identical irradiation conditions (except for the recoil energy), the observed difference in the damage accumulation behaviour directly demonstrates that cascades play a significant role in the damage accumulation processes and that the efficiency of damage accumulation is likely to depend on recoil energy.

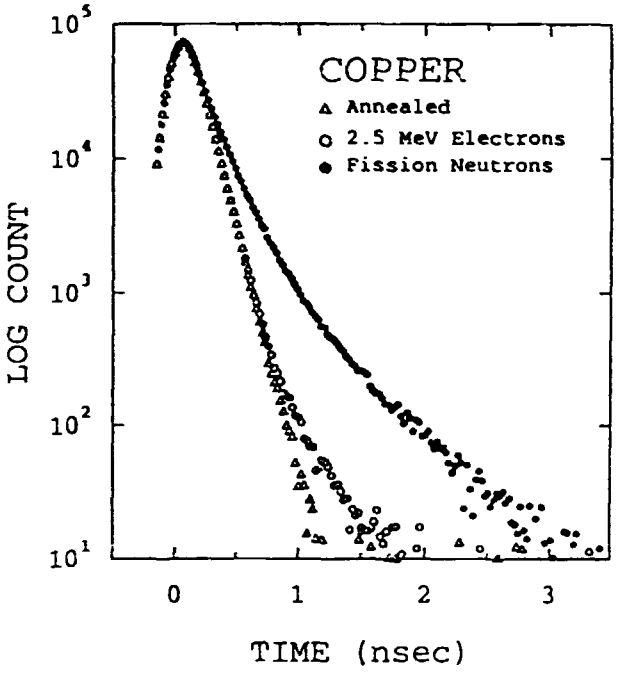


*Figure 2. Positron lifetime spectra for copper: Well annealed (Δ) and irradiated at ~523 K with neutrons to 0.01 dpa (•), and by electrons to 0.013 dpa (o).*

### 3.1.2 Effect of Fission Neutron and 600 MeV Proton Irradiations on Microstructural Evolution in Copper

(B.N. Singh and A. Horsewell)

During irradiation of copper with 14 MeV neutrons in a fusion device, most of the displacement damage would occur in the form of cascades and subcascades. Concurrently, nuclear reactions would produce (a) helium at a relatively high rate and (b) additional transmutational impurities (solid) to those produced under fission neutron irradiations. Although the production of cascades and subcascades in themselves may not enhance the cavity formation, the higher rate of helium production is likely to increase the cavity density in the grain interior as well as the helium accumulation at grain boundaries. In order to evaluate the effects of the helium generation rate and recoil energy, we have irradiated pure copper with fission neutrons and 600 MeV protons. The rate of helium production during fission neutron irradiation is ~0.15 appm/dpa, whereas 600 MeV proton irradiation produces helium at a rate of ~125 appm/dpa.

Specimens of OFHC-copper were irradiated with fission neutrons in the DR-3 reactor at Risø in the high temperature rig where the temperature of the magazine containing specimens is measured and controlled continuously. Irradiations were carried out at 523 K to fluence levels of $5\times10^{23}$ n/m$^2$ and $1.5\times10^{24}$ n/m$^2$ (E>1 MeV), corresponding to displacement dose levels of 0.1 and 0.3 dpa, respectively. Specimens of the same material were irradiated with 600 MeV protons at 623 and 673 K in the PIREX facility at PSI (Switzerland).

The main features of the post-irradiation microstructure were investigated using TEM. The results on microstructural parameters are given in Table 2. The results clearly demonstrate that the damage accumulation behaviour during 600 MeV proton irradiation is significantly different from that observed under fission neutron irradiation. There are two outstanding examples of such differences. First, the irradiations with 600 MeV protons at 623 and 673 K yield a significantly higher cluster density than that in the fission neutron irradiated copper (also see section 3, Fig. 4). Second, a complete absence of cavity formation is found in the OFCH-copper irradiated to ~0.5 dpa with 600 MeV protons even at 623 K whereas void nucleation and growth are observed to occur quite readily during neutron irradiation of the same copper already at 523 K and at dose level of as low as ~0.001 dpa (see section 1).

**Table 2: Microstructural parameters (i.e. void concentration $C_v$, mean void size, $\bar{d}_v$, swelling $S_v$, and total cluster density, $C_{ci}$ for grain interiors in copper irradiated with fission neutrons and 600 MeV protons.**

| Particles | Dose (dpa) | $T_{irr}$ (K) | $C_v$ ($m^{-3}$) | $\bar{d}$ (nm) | $S_v$ (%) | $C_{cl}$ ($m^{-3}$) |
|---|---|---|---|---|---|---|
| Neutrons | ~0.1 | 523 | $4.16\times10^{20}$ | 14.6 | 0.06 | $5.5\times10^{22}$ |
| " | ~0.3 | 523 | $6.13\times10^{20}$ | 16.1 | 0.13 | $6.8\times10^{22}$ |
| " | ~1.3 | 523 | $1.6\times10^{20}$ | 28 | 0.23 | $8.0\times10^{22}$ |
| " | ~1.2 | 623 | $3.8\times10^{19}$ | 49 | 0.35 | $2.2\times10^{21}$ |
| 600 MeV | ~0.5 | 623 | - | - | - | $1.2\times10^{23}$ |
| Protons | ~0.5 | 673 | $2.5\times10^{18}$ a) | 111 a) | 0.18 | $5.7\times10^{21}$ |
| | | | $2.0\times10^{19}$ b) | 45 b) | 0.09 | |

(a) large (b) small cavities in the dual size distribution.

These differences are interpreted to arise from two sources. The high energy recoils in the case of 600 MeV proton irradiation are likely to be more efficient in generating intracascade clusters (hence higher cluster density). The high helium generation rate during 600 MeV proton irradiation is likely to cause nucleation of small helium bubbles and may stabilize the stacking fault tetrahedra formed in cascades and subcascades. Both these factors are likely to cause a rapid build-up of a high sink strength. This would reduce the level of vacancy supersaturation drastically. Hence, the lack of visible cavities and the absence of swelling.

In the OFHC-copper irradiated with fission neutrons at 523 K the void swelling was found to be significantly enhanced (i.e. compared to the smelling in the grain interior) in a relatively wide zone immediately adjacent to grain boundaries. Fig. 3 shows the variation of void size and swelling with the distance from a grain boundary for a dose level of ~0.3 dpa. This behaviour can be understood in terms of the production bias model (see section 9).

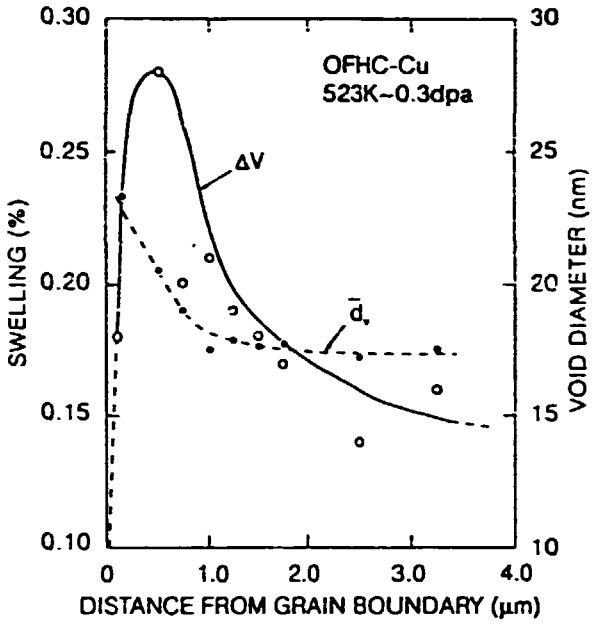


*Figure 3. Variation of void swelling and size with distance away from a grain boundary in copper irradiated with neutrons at 523 K to 0.3 dpa.*

### 3.1.3 Defect Microstructure in Copper Alloys Irradiated with 750 MeV Protons

(S.J. Zinkle (Oak Ridge National Laboratory, USA), A. Horsewell, B.N. Singh, and W.F. Sommer (Los Alamos National Laboratory, USA))

The microstructural evolution in copper and its alloys during neutron irradiation at low to moderate temperatures and doses (373-473K, 0.1 to 10 dpa) is not well established. The role of solid solution alloying additions in the microstructural evolution is not well understood either. The present study compares the microstructural response of pure copper and three binary alloys containing 5 at.% of either Al, Mn or Ni.

The TEM discs (3 mm in diameter) were irradiated with 750 MeV protons at the Los Alamos Meson Physics Facility (LAMPF) at irradiation temperatures in the range 333 K to 473 K to displacement dose levels in the range 0.5 to 2.5 dpa.

The dominant radiation-induced microstructural feature observed in all of the copper specimens was a high density of small defect clusters. The defect cluster density was independent of dose and temperature for copper specimens irradiated between 0.4 dpa, 333 K and 1 dpa, 403 K, with a value of $1.2 \times 10^{24}/m^3$. The defect cluster density decreased gradually with increating temperature for irradiations performed above 423 K (Fig. 4). Fig. 4 also includes the results of fission neutron and 600 MeV proton irradiations (section 2). These results clearly suggest that the temperature dependence of the cluster density is shifted significantly towards higher temperatures for irradiation conditions dominated by high energy recoils.

Cavity formation was only observed in copper specimens irradiated at relatively high doses and temperatures. A high density ($\sim 6 \times 10^{22}$ $m^3$) of small cavities (~1.8-2.5 nm diameter) was observed in the grain interiors of copper specimens irradiated to dose levels of greater than 1.5 dpa at temperatures > 423 K.

Solute additions of the order of 5 at.% do not seem to have any significant effect on the overall probability of an energetic displacement cascade collapsing to form

an observable defect cluster. However, the fraction of resolvable SFTs is considerably reduced by solute additions, including solutes which reduce the macroscopic stacking fault energy of copper. Solute additions can significantly enhance the interstitial dislocation loop concentration in pure copper. This enhancement occurs even for solute additions such as Ni which, in solid solution, do not have a strong binding to SIAs.

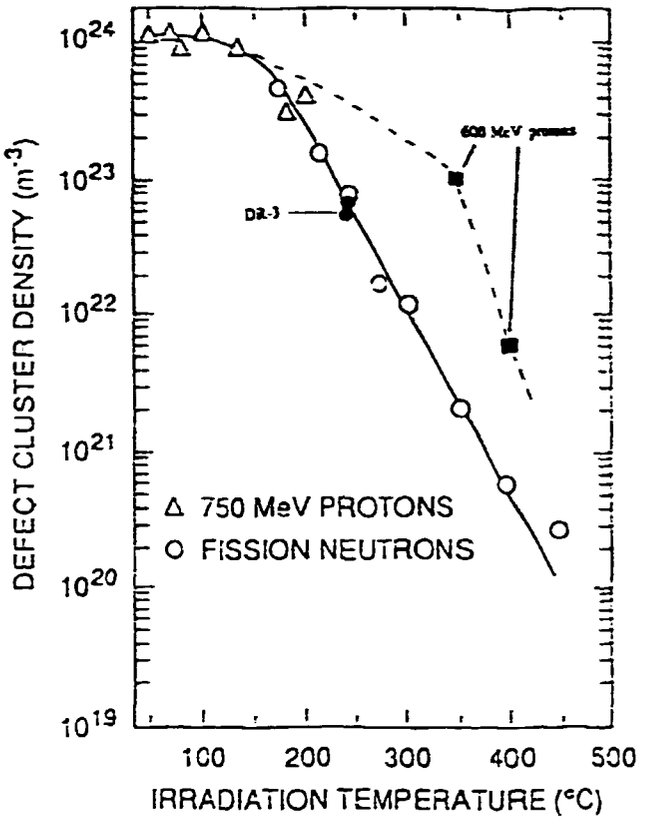


*Figure 4. Temperature dependence of cluster density in copper irradiated with neutron (o●), 750 MeV protons (Δ) and 600 MeV protons (□).*

### 3.1.4 Effect of Neutron Irradiation on Tensile Properties of Copper and Copper Alloys

(B.N. Singh, A. Horsewell, and P. Toft)

Copper and its alloys are attractive for applications in fusion reactor systems (e.g. NET and ITER) because of their excellent thermal conductivity. In the past, a large number of investigations have been reported on effects of irradiations on defect accumulation in copper. However, the amount of experimental results available on the evolution of defect microstructure and its impact on deformation behaviour is rather limited particularly at temperatures in the range of interest for NET and ITER (e.g. ~300-700 K).

To investigate the influence of irradiation-induced microstructure on mechanical performance, a number of tensible specimens of copper, $Cu - Al_2O_3$, $CuCrZr$, and $CuNiBe$ alloys were irradiated with fission neutrons to doses in the range $10^{-3} - 3 \times 10^{-1}$ dpa at ~320 K. In addition, tensile specimens of copper were irradiated at 523 K also in the dose range of $10^{-3} - 3 \times 10^{-1}$ dpa. The specimens

of copper and copper alloys irradiated at ~320 K were tensile tested at 295 K. The dose dependencies of the yield strength and ultimate tensile strength for copper and copper alloys are shown in Fig.5. It is interesting to note that the variation of tensile strengths with neutron fluence for copper and $Cu - Al_2O_3(CuAl25)$ is quite different from that for *CuCrZr* and *CuNiBe* alloys. In order to find out the reason for this difference, the microstructure of these materials is being investigated. It should be pointed out that both total and uniform elongations for copper and copper alloys decrease with increasing neutron fluence. Unfortunately, the uniform elongation in all irradiated copper and copper alloys reaches a value of about 0.2% already at a relatively low dose of ~0.2 dpa. This implies that even low dose irradiation at about 320 K causes so much damage accumulation in copper and copper alloys that these materials are no longer able to deform plastically.

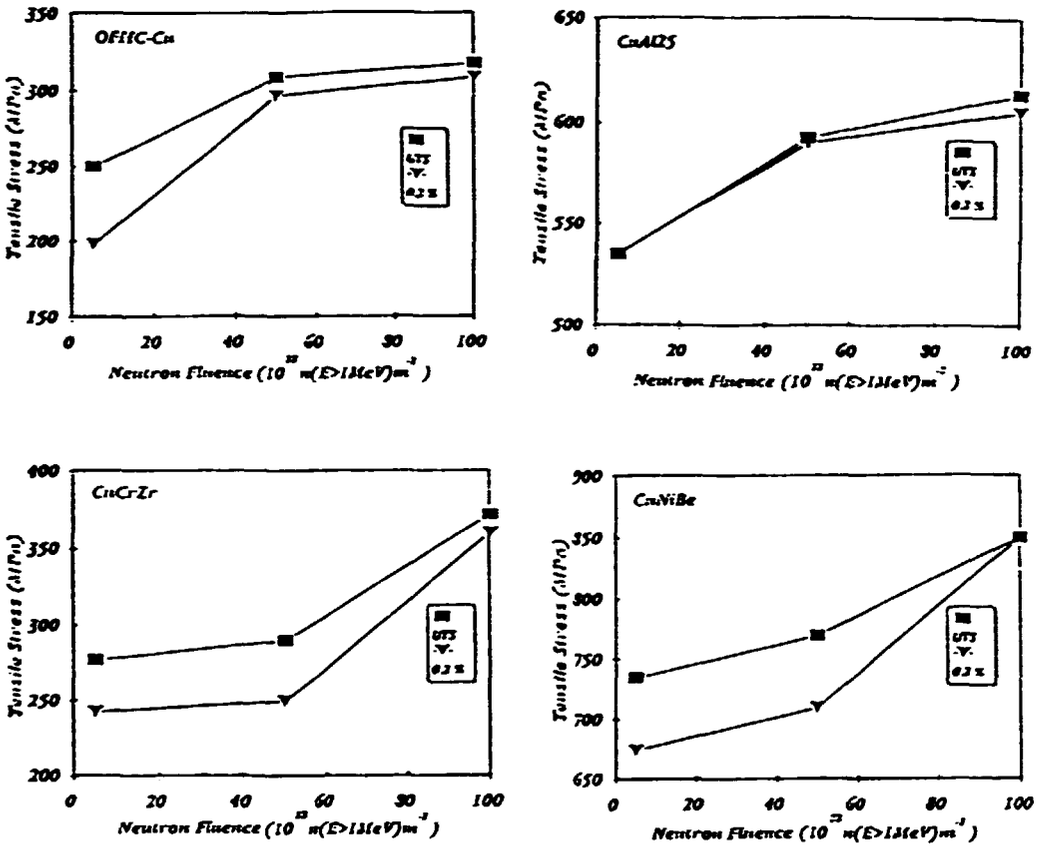


*Figure 5. Variation of tensile strength with neutron fluence in copper, CuAl25, CuCrZr, and CuNiBe alloys irradiated at ~320 K and tested at 295 K.*

### 3.1.5 Effect of Neutron Irradiation on Microstructure and Mechanical Properties of TZM and Mo-5% Re Alloys

(B.N. Singh, A. Horsewell, P. Toft, and J.H. Evans (University of London, England))

Investigations of the effect of neutron irradiation on microstructural evolution and mechanical properties of molybdenum alloys have been continued. Tensile specimens of TZM and Mo-5% Re alloys were irradiated with fission neutron to a fluence of ~ $1.5 \times 10^{24}$ n/m$^2$ (E>1MeV); this fluence level corresponds to a displacement dose of ~0.16 dpa. Irradiations have been carried out at 320, 373,

523, 623, and 723 K. Both unirradiated and irradiated specimens were tensile tested at 295 and 373 K. Tensile testings of specimens irradiated at 523, 623, and 723 K are in progress. Results of tensile tests at 295 and 373 K are summarized in Table 3 and some examples of stress-strain curves for irradiated and unirradiated materials are shown in Fig. 6.

The results show that Mo-5% Re alloy is stronger and less ductile than TZM. A surprising result is that at 373 K the strength is higher and the elongation is lower than that at 295 K for the unirradiated TZM and Mo-5% Re alloys; the irradiated materials, on the other hand, exhibit the normal behaviour (i.e. higher strength at lower temperature). As clearly demonstrated by the results shown in Fig. 6 and Table 3, the irradiation to a dose level of only ~0.16 dpa increases the strenght of TZM and Mo-5% Re alloys by a factor of almost two and reduces the ductility of these materials to practically zero.

Specimens of TZM and Mo-5% Re alloys irradiated at ~320, 373, 523, and 623 K were investigated for the irradiation-induced changes in the microstructure. The TEM examinations showed the presence of high densities of small defect clusters and loops at ~320 and ~373 K (Table 4). There were clear indications of early stages of loop rafting in TZM specimens irradiated at ~320 as well as ~373 K. No such indications were observed in Mo-5% Re specimens irradiated at ~320 and ~373 K. In TZM specimens irradiated at 523 and 623 K, the dislocation microstructure was dominated by clusters and rafts of loops, with a general (111) habit plane. In the Mo-5% Re alloy, on the other hand, the microstructure even at 523 and 623 was dominated by high densities of small loops.

Table. 3. Average values of 0.2% yield strength ($\sigma_{0.2}$), ultimate tensile strength $\sigma_{uts}$, uniform elongation ($\varepsilon_u$) and total elongation ($\varepsilon_t$) for TZM and Mo-5%Re alloys

| Materials | Condition | $T_{irr}$ (K) | $T_{test}$ (K) | $\sigma_{0.2}$ (MPa) | $\sigma_{uts}$ (Mpa) | $\varepsilon_u$ (%) | $\varepsilon_t$ (%) |
|---|---|---|---|---|---|---|---|
| TZM | unirradiated | - | 295 | 439 | 504 | 11.00 | 17.00 |
| | unirradiated *) | - | 295 | 503 | 552 | 11.00 | 19.57 |
| | irradiated | 320 | 295 | - | 1127 | 0.32 | 0.35 |
| | unirradiated | - | 373 | 490 | 640 | 3.45 | 4.22 |
| | irradiated | 373 | 373 | - | 950 | 0.35 | 0.65 |
| Mo-5%Re | unirradiated | - | 295 | 575 | 706 | 6.00 | 7.00 |
| | unirradiated *) | - | 295 | 798 | 927 | 7.20 | 10.20 |
| | irradiated | 320 | 295 | - | 1425 | 0.28 | 0.29 |
| | unirradiated | - | 373 | 920 | 934 | 0.70 | 1.02 |
| | irradiated | 373 | 373 | - | 1239 | 0.30 | 0.32 |

*)tested in unpolished condition (i.e. with as-fabricated surfaces)

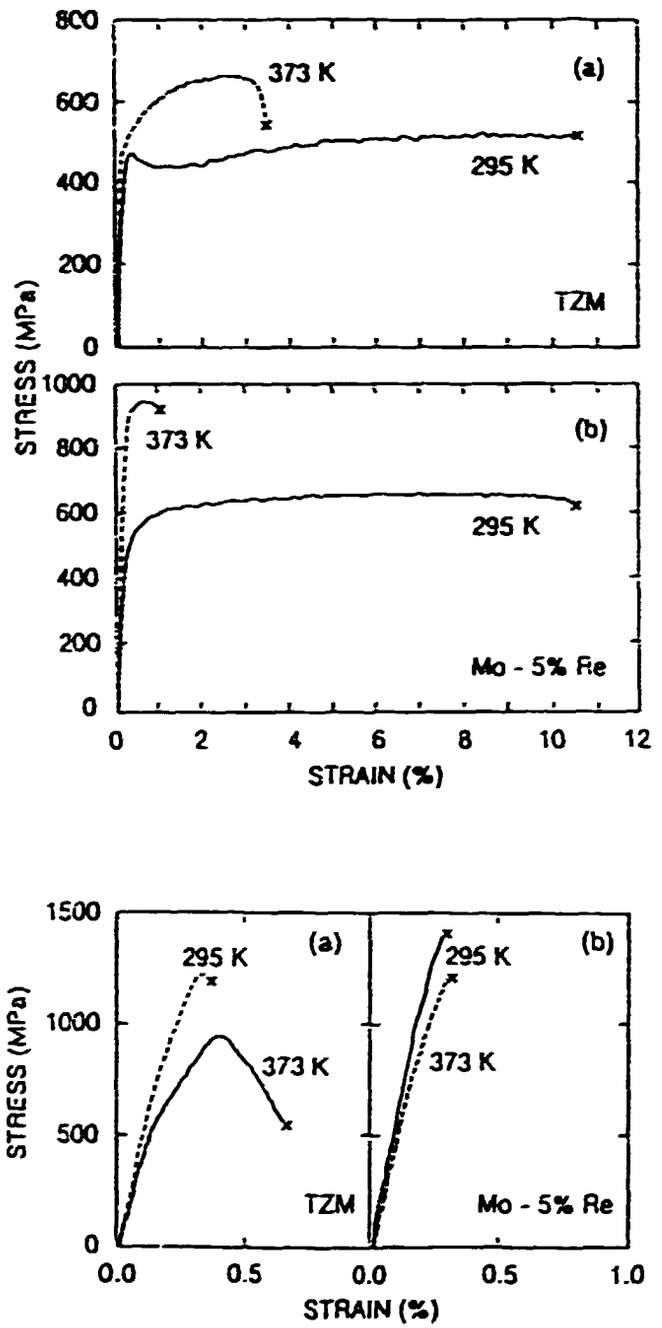


*Figure 6. Stress-strain curves for TZM and Mo-5% Re alloy tested in unirradiated (top) and irradiated (bottom) conditions at 295 and 373 K after irradiation at ~320 and 373 K, respectively.*

**Table 4. Loop densities ($C_l$) and Sizes ($d_l$) for TZM and Mo-5% Re alloys irradiated to a dose level of ~0.16 dpa.**

| Material | Irradiation Temperature (K) | $C_l$ ($m^{-3}$) | $d_l$ (nm) |
|---|---|---|---|
| TZM | 320 | $1 \times 10^{23}$ | 3.3 |
| " | 373 | $4 \times 10^{22}$ | 4.0 |
| " | 523 | $5 \times 10^{21}$ | 50*) |
| " | 623 | $1 \cdot 6 \times 10^{21}$ | 75*) |
| Mo-5% Re | 320 | $1 \times 10^{23}$ | 2.5 |
| " | 373 | $8 \times 10^{22}$ | 3.1 |
| " | 523 | $4 \cdot 8 \times 10^{22}$ | 3.2 |
| " | 623 | $1 \cdot 2 \times 10^{22}$ | 3.2 |

*) refers to clusters/rafts of loops and not single loops.

TEM examinations of TZM specimens irradiated at 623 K revealed the presence of a high density ($3 \cdot 8 \times 10^{23}$ $m^{-3}$) of small voids (0.75 nm diameter). The presence of voids in the Mo-5% Re alloy irradiated at 623 K could not be clearly established.

Fracture surfaces in TZM and Mo-5% Re alloys tensile tested at 295 and 373 K in irradiated as well as unirradiated conditions were examined in an Electroscan Environmental scanning electron microscope (ESEM). In most cases the fracture surface shows transgranular cleavage, except for the unirradiated TZM tested at room temperature where there is an indication of some plastic deformation in the grains. The main feature of the deformation mode in these materials seems to be grain boundary sliding and separation, indicating that the grain boundaries are *much weaker than the grains. Thus, the main source of the irradiation-induced* embrittlement appears to be the exhaustion of plastic deformability of the grains and grain boundary weakness and not grain boundary embrittlement caused by irradiation)induced segregation, as is commonly assumed.

### 3.1.6 Effect of Cold-Work on Void Swelling Under Fission Neutron Irradiation

(H. Watanabe (Kyushu University, Japan), F.A. Garner (Pacific Northwest Laboratory, USA), and B.N. Singh)

In technological applications, for example, as structural materials in divertor components, copper and copper alloys are likely to be used in cold-worked state. Some years ago it was shown that during electron irradiation, the void swelling was found to increase with increasing level of cold work reaching a maximum at 50% cold-work level. In order to determine whether or not the effect of cold-work on void swelling will be similar under neutron irradiation conditions, a number of cold-worked specimens were irradiated with fission neutrons in the Fast Flux Test Facility (FFTF). Specimens were obtained from the same batch of pure copper used in the electron irradiations. Irradiations were carried out at 638 and 706 K to doses of 16.9 and 47.3 dpa, respectively.

Fig. 7 shows the variation of swelling with the cold-work level; the swelling

was determine by density change measurements. As can be readily seen, during neutron irradiations at 638 and 706 K, the swelling does not increase with cold-work; instead, the swelling is reduced noticeably already at the 10% cold)work level and is found to remain at this reduced level at the higher cold-work levels up to 50%. The reason for this difference in the effect of cold-work on swelling between electron and neutron irradiations is not very obvious. To help understand this effect, irradiated specimens will be investigated using TEM.

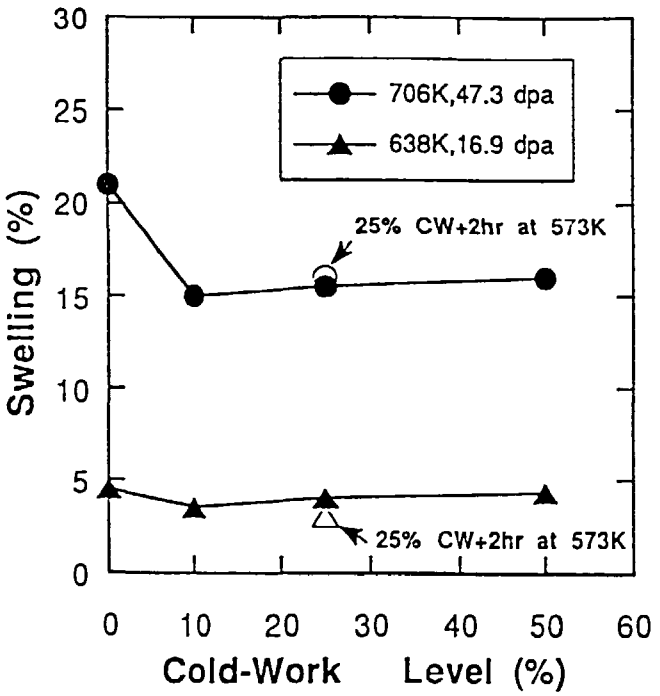


*Figure 7. Effect of Cold-Work on void swelling in copper irradiated at 638 and 706 K to 16.9 and 47.3 dpa, respectively.*

### 3.1.7 Thermal Annealing Behaviour of Helium Bubbles in Copper Studied by Positron Annihilation Technique

(M. Eldrup, B.N. Singh, and A. Möslang (Kernforschungszentrum, Karlsruhe, Germany))

The positron annihilation technique (PAT) is a useful supplementary technique to the transmission electron microscopy (TEM) in studies of defects and defect clusters in metals. Positrons injected into a metallic sample become attracted to vacancy type defects such as dislocations, vacancies, vacancy clusters, voids and bubbles and may become trapped at such defects. By proper measurements (e.g. of the lifetime of the positrons) defect characteristic parameters may be obtained.

Taking advantage of the fact that PAT is a non-destructive technique, PAT studies have been carried out of the annealing behaviour of specimens Cu which were implanted with He at different temperatures and to different He concentrations (and rates). Some of the results for two of the specimens are shown in Fig. 8.

The lifetime $\tau_3$ of positrons trapped in bubbles depends both on the bubble

size, the He density in the bubbles and may also be sensitive to impurities on the bubble surfaces. For bubbles big enough to be seen by TEM the lifetime is size independent.

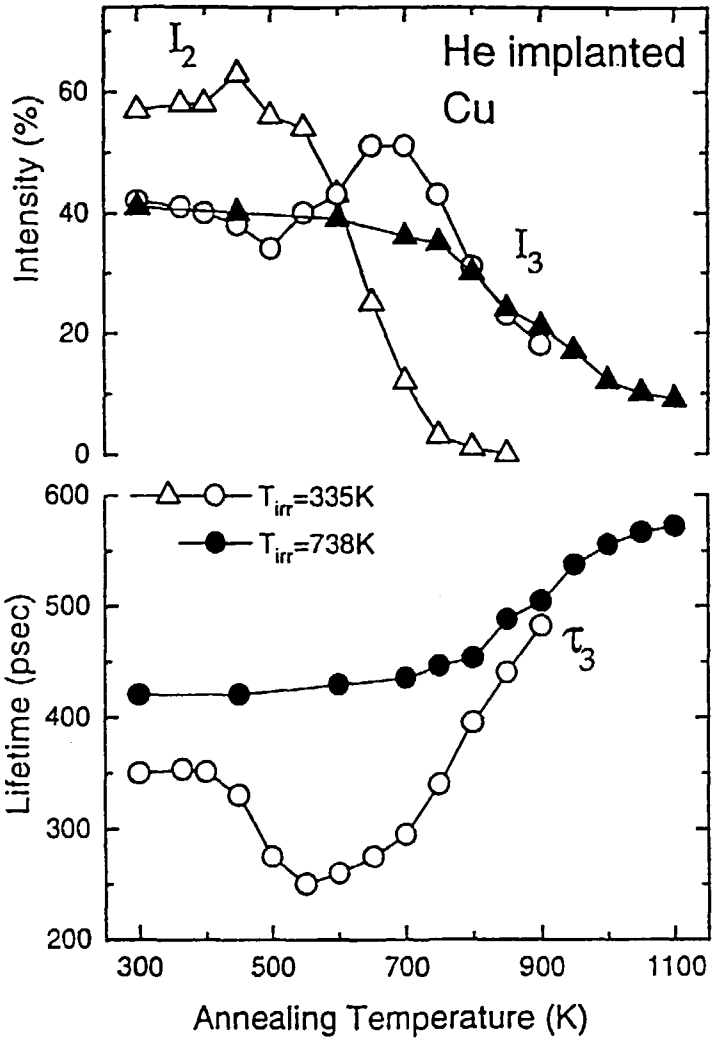


*Figure 8. The longest positron lifetime, $\tau_3$, which is ascribed to positrons trapped in He bubbles, and its intensity, $I_3$, as functions of annealing temperature for Cu implanted 1) at 738 K to a concentration of 341 appm He, sample K9 (closed symbols) and 2) at 335 K to a concentration of 108 appm He, sample K3 (open symbols). The intensity, $I_2$, of a component with lifetime $\tau_2$ = 185 picosec (ps) is also shown for sample K3. This component is ascribed to positrons trapped at dislocations and small vacancy-He clusters.*

For the as-implanted specimen K9 (bubble diameter = 5.8 nm from TEM), the average He density in the bubbles is found to be $3.1 \times 10^{28}$ $m^{-3}$ (if impurity effects can be ignored). On annealing, the lifetime increases and its intensity decreases with increasing annealing temperature above about 600K. This shows that coalescence of bubbles starts to take place and that the He density in the bubbles decreases, i.e. the swelling increases. At the highest annealing temperatures $\tau_3$ becomes longer than the 500 ps expected for a pure void surface, indicating that the bubble surface has been contaminated, maybe by oxygen.

For the low-temperature implanted specimen K3, the lifetime component as-

sociated with dislocations and small He-vacancy clusters ($I_2$) anneals out in the range 550-800 K as expected for dislocation loops. No bubbles can be seen in TEM in the as implanted specimen in agreement with the low value of $\tau_3$ which is characteristic for clusters containing a few vacancies (5-10) and/or a high density of He (less than $6 \times 10^{28}$ $m^{-3}$). The strong decrease in this lifetime at about 500 K is the signature of defect reactions, maybe the dissociation of some vacancies from the clusters. At higher temperatures the increase in lifetime again indicates the coalescence and growth of bubbles with a simultaneous drop in He density within the bubbles.

After the final anneal the specimens will be examined by TEM to establish a direct correlation between positron trapping rates and bubble densities and sizes for Cu.

### 3.1.8 A Multi-Model Approach to Study Defect Production in High Energy Collision Cascades

(H.L. Heinisch (Pasific Northwest Laboratory, USA) and B.N. Singh)

A multi-model approach is being employed to simulate defect production processes at the atomic scale. The model incorporates molecular dynamics (MD), binary collision approximation (BCA) calculations and stochastic annealing simulations. The central hypothesis is that the simple, fast computer codes capable of simulating large numbers of high energy cascades (e.g. BCA codes) can be made to yield the correct configurations when their parameters are properly calibrated using the results of the physically more realistic MD simulations. The calibration procedure has been investigated using results of MD simulations of 25 keV cascades in copper. The configurations of point defects are extracted from MD cascades simulations at the end of the collisional phase, thus providing information similar to that obtained with a binary collision model. The MD collisional phase defect configurations are used as input in the ALSOME annealing simulation code. The values of the ALSOME quenching parameters are determined that yield the best fit to the post-quenching defect configurations of the MD simulations. A set of 100 cascades of 25 keV was produced in copper with the BCA code MARLOWE and run through the ALSOME quenching and short term annealing. The yields of total and freely migrating defects in these simulations were very similar to those obtained in the MD cascades after short term annealing. The SIA cluster distribution after short term annealing, starting from both the quenched standard and the collisional stage are shown in Fig. 9. It should be pointed out that the large SIA clusters produced during the quenching stage in the MD simulation of cascades were not produced as frequently in the present short-term annealing with ALSOME. This may be due primarily to the assumption used in ALSOME that all defect migration occurs by uncorrelated jumps.

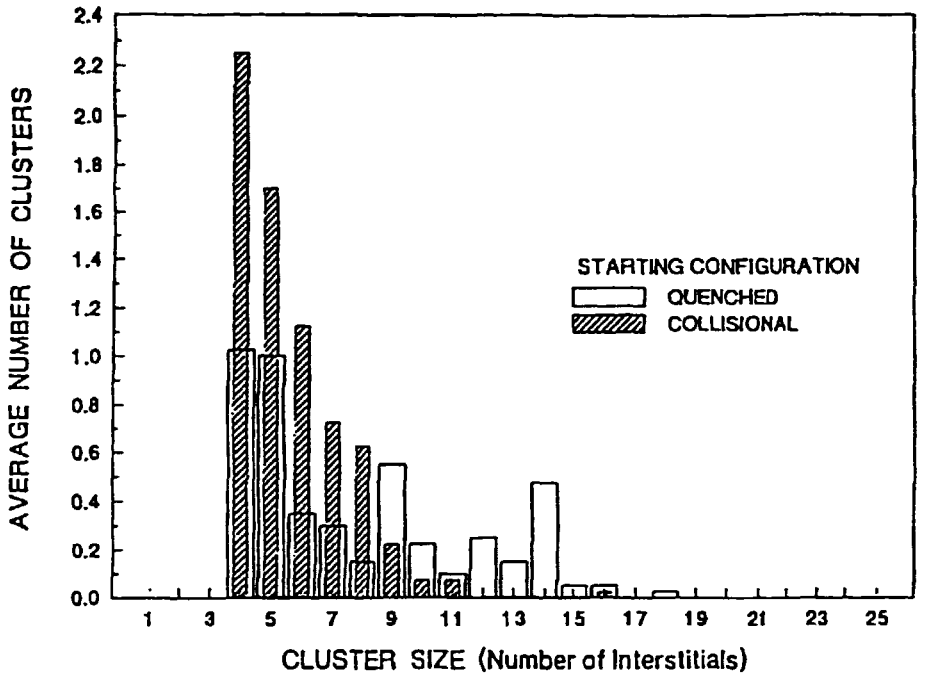


*Figure 9. Interstitial cluster size distributions after short-term annealing with the annealing code ALSOME for a time and temperature at which single vacancies diffuse, for 25 KeV cascades in copper. The open bars are for the average final configuration of 100 anneals when starting form the quenched cascades form MD. The striped bars are for 100 anneals when starting form the collisional stage in MD, i.e. when both the quenching and short-term annealing stages are simulated with ALSOME.*

### 3.1.9 Application of Production Bias Model to Study Damage Accumulation Under Cascades Damage Conditions

(H. Trinkaus (Forschungszentrum Jülich, Germany), B.N. Singh, and A.J.E. Foreman (Harwell Laboratory, England))

The concept of production bias is based on the fact that under cascades damage conditions a substantial fraction of SIAs and vacancies are produced in the form of clusters. The fact that SIA clusters are thermally stable in the void swelling temperature range and vacancy clusters evaporate very rapidly, gives rise to an asymmetry in the production of SIAs and vacancies. It has been shown that this asymmetry (i.e. the production bias) would become a potent driving force for void swelling if a significant fraction of the stable SIA clusters produced in the cascades were annihilated preferentially at extended sinks such as dislocations and grain boundaries. Both MD simulations and experimental results suggest that the removal of small SIA clusters is likely to occur via one-dimensional glide. Over the years, a large number of experimental observations have been reported showing repeatedly that void swelling is significantly enhanced in a relatively wide zone adjacent to grain boundaries. Furthermore, this enhancement occurs only under cascade damage conditions. Calculations have shown that these observations can not be understood in terms of conventional rate theory using dislocation bias

for monointerstitials as the only driving force. Recently, we have calculated the swelling behaviour in this zone as a function of distance from the grain boundary using the production bias model and removal of SIA clusters by one-dimensional (1D) glide.

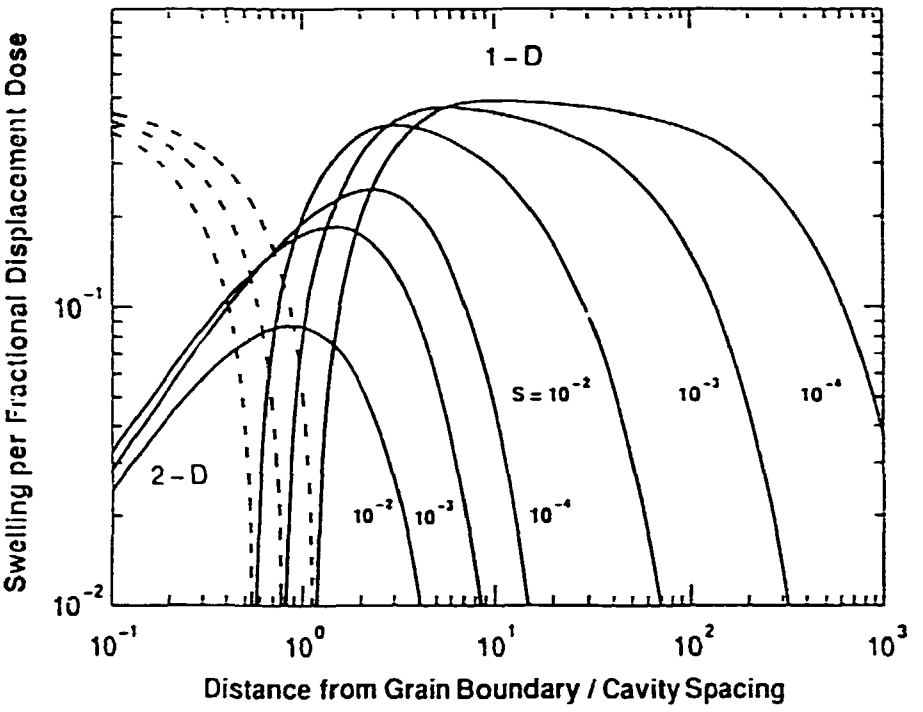


*Figure 10. Variation of swelling rate with distance away from a grain boundary calculated for copper neutron irradiated at 523 K assuming three different swelling levels.*

Fig. 10 shows the variation of calculated smelling rate with the distance from a grain boundary for 1D as well as 2D interstitial transport for three different swelling levels. Both the position of the peak swelling rate and the total width of the zone where swelling is enhanced (compared to swelling in the grain interior) are in very good agreement with the experimental results. The width of the peak swelling zone is found to be approximately equal to the mean range (of SIA cluster escape) corresponding to the peak swelling. This is yet another indication which would suggest that the production bias is a realistic model to describe the damage accumulation under cascade damage conditions.

## 3.2 Water Radiolysis under NET/ITER Conditions

### 3.2.1 NET Technology Programme subtask NWC1-1

Progress Report 1993 (E. Bjergbakke)

**Stage I, item 1.**
Further consideration has been given to the problem of the G-value limit for water-decomposition.
**Stage I, item 2 and 3.**
Simulations will be done as soon as the experimental results at 200°C are available.

## 3.3 Participants in the Fusion Technology Work

**Scientific Staff**
Bjergbakke, E. (part-time < 10%)
Eldrup, Morten (part-time, ~50%)
Horsewell, Andy (part-time, ~20%)
Johansen, B.S. (part-time, ~20%)
Singh, Bachu N.
Toft, Palle (part-time, ~20%)

**Technical Staff**
Lindbo, Jørgen (part-time, ~10%)
Nilsson, Helmer (part-time, ~10%)
Olsen, Benny F.
Pedersen, Niels Jørgen (part-time, ~30%)

**Guest Scientists**
Evans, J.H., University of London, England
Woo, C.H., Atomic Energy of Canada Ltd., Pinawa, Canada

**Short Time Visitors**
Szenes G., Eötvös University, Budapest, Hungary
Heinisch, H.L., Pacific Northwest Laboratories, Richland, USA
Edwards, D.J., Pacific Northwest Laboratories, Richland, USA

## 3.4 Publications and Conference Contributions

### 3.4.1 Publications


Bacon, D.J., Gavillet, D., Horsewell, A., Ishino, S., Mansur, L.K., Singh, B.N., Trinkaus, H., Ullmaier, H., Victoria, M. (1993). Summary of Montreux workshop on time dependence of radiation damage accumulation and its impact on materials properties. J. Nucl. Mater. v. 206 p. 368-371.

Garner, F.A., Edwards, D.J., Singh, B.N., Watanabe, H. (1993). Neutron induced swelling observed in copper alloys irradiated in MOTA's 2A and 2B. In: Fusion reactor materials. Semiannual progress report for period ending March 31, 1993. DOE-ER-0313-14, p. 345-346.

Garner, F.A., Hamilton, M.L., Stubbins, J.F., Singhal, A., Singh, B.N. (1993). Status of fatigue studies on irradiated copper alloys. In: Fusion reactor materials. Semiannual progress report for period ending March 31, 1993. DOE-ER-0313-14 p. 127-140.

Garner, F.A., Singh, B.N. (1993). The influence of cold work level on swelling of pure copper irradiated by fast neutrons or electrons. In: Fusion reactor materials. Semiannual progress report fo period ending March 31, 1993. DOE-ER-0313-14. p. 127-140.

Gavillet, D., Victoria, M., Singh, B.N., Horsewell, A. (eds.). (1993). Time dependence of radiation damage accumulation and its impact on materials properties. Workshop, Montreux (CH), 14-20 Oct. 1992. (North-Holland, Amsterdam, 1993) (Journal of Nuclear Materials, vol. 206, nos. 2/3) 267 p.

Hegedüs, F., Wobrauschek, P., Sommer, W.F., Ryon, R.W., Streli, C., Winkler, P., Ferguson, P., Kregsamer, P., Rieder, R., Victoria, M., Horsewell, A. (1993). Total reflection X-ray flourescence spectrometry of metal samples using synchrotron radiation at SSRL. X-Ray Spectrom. v. 22 p. 277-280.

Heinisch, H.L., Singh, B.N.,(1993) On the structure of irradiation-induced collision

cascades in metals as a function of recoil energy and crystal structure, Phil. Mag. v. A67 p. 407-424.

Horsewell, A., Alurralde, M., Caro, A., Victoria, M. (1993). Simulation of thin foils and bulk irradiations: Recoil emission from surfaces and thermal spike effects. J. Phys. Condens. Matter v. 5 p. A281-A282

Singh, B.N., (1993) Consequences of radiation)produced interstitials, vacancies and gas atoms: Void swelling. In: Lecture notes from the international summer school on the fundamentals of radiation damage. Vol. 2. International summer school on the fundamentals of radiation damage. University of Illinois, Urbana-Champaign, IL (US), 1-2 Aug 1993. (Frederik Seitz Materials Research Laboratory, University of Illinois, Urbana-Champaign, IL, 1993) 33 p.

Singh, B.N., Zinkle, S.J. (1993). Defect accumulation in pure fcc metals in the transient regime: A review. J. Nucl. Mater. v. 206 p 212-229.

Trinkaus, H., Singh, B.N., Foreman, A.J.E., (1993). Impact of glissile interstitial loop production in cascades on defect accumulation in the transient. J. Nucl. Mater. v. 206 p. 200-211.

Woo, C.H., Semenov, A.A., Singh, B.N., (1993). Analysis of microstructural evolution driven by production bias. J. Nucl. Mater. v. 206 p. 170-199.

Zinkle, S.J., Singh, B.N. (1993). Analysis of displacement damage and defect production under cascade damage conditions. In: Fusion reactor materials. Semiannual progress report for period ending September 30, 1992. DOE-ER-0313-13 (1992) p. 55-73.

Zinkle, S.J., Singh, B.N. (1993). Analysis of displacement damage and defect production under cascade damage conditions. J. Nucl. Mater. v. 199 p. 173-191.

### 3.4.2 Conference Contributions

Heinisch, H.L., Singh, B.N., and Diaz de la Rubia, T. (1993). Calibrating a multimodel approach to defect production in high energy collision cascades, 6th International Conference on Fusion Reactor Materials, Stresa, Italy (September-October).

Singh, B.N. and Horsewell, A. (1993). Effects of 600 MeV proton and fission neutron irradiations on microstructural evolution in OFHC-copper, 6th International Conference on Fusion Reactor Materials, Stresa, Italy (September-October).

Singh, B.N. and Zinkle, S.J. (1993). Influence of irradiation parameters on damage accumulation in metals and alloys, 6th International Conference on Fusion Reactor Materials, Stresa, Italy (September-October).

Singh, B.N. and Trinkaus, H. and Woo, C.H. (1993). Production bias and cluster annihilation: Why necessary?, 6th International Conference on Fusion Reactor Materials, Stresa, Italy (September-October).

Singh, B.N., Horsewell, A. Toft, P. and Evans, J.H. (1993). Effect of neutron irradiation on microstructure and tensile properties of TZM and Mo-5% Re alloys, 6th International Conference on Fusion Reactor Materials, Stresa, Italy (September-October).

Singhal, A., Stubbins, J.F., Singh, B.N. and Garner, F.A. (1993). Room temperature fatigue behaviour of OFCH copper and CuAl 25 specimens of two sizes, 6th International Conference on Fusion Reactor Materials, Stresa, Italy (September-October).

Watanabe, H., Garner, F.A. and Singh, B.N. (1993). Void swelling in pure copper, Cu-5Ni and Cu-5Mn alloys, 6th International Conference on Fusion Reactor Materials, Stresa, Italy (September-October).

Zinkle, S.J., Horsewell, A., Singh, B.N. and Sommer, W.F. (1993). Defect microstructure in copper alloys irradiated with 750 MeV protons, 6th International Conference on Fusion Reactor Materials, Stresa, Italy (September-October).

**Bibliographic Data Sheet** **Risø-R-761(EN)**

Title and author(s)

ANNUAL PROGRESS REPORT 1993

Work in Controlled Thermonuclear Fusion Research Performed in The Fusion Research Unit under the Contract of Association between Euratom and Risø National Laboratory

edited by L. Astradsson and V.O. Jensen


| ISBN | ISSN |
|---|---|
| 87-550-2000-3 | 0106-2840 |

| Dept. or group | Date |
|---|---|
| Optics and Fluid Dynamics Department | September 1994 |

| Groups own reg. number(s) | Project/contract No. |
|---|---|
| | |

| Pages | Tables | Illustrations | References |
|---|---|---|---|
| 50 | 4 | 21 | 64 |



Abstract (Max. 2000 char.)

The programme of the Research Unit of the Fusion Association Euratom-Risø National Laboratory covers work in fusion plasma physics and in fusion technology. The fusion plasma physics group has activities within (a) studies of nonlinear dynamical processes in magnetized plasmas, (b) development of pellet injectors for fusion experiments, and (c) development of diagnostics for fusion plasmas. The activities in technology cover radiation damage of fusion reactor materials. A summary of the activities in 1993 is presented.



Descriptors INIS/EDB

COHERENT SCATTERING; EDGE LOCALIZED MODES; JET TOKAMAK; MAGNETIC CONFINEMENT; NONLINEAR PROBLEMS; PARAMETRIC INSTABILITIES; PELLET INJECTION; PLASMA DIAGNOSTICS; PLASMA SCRAPE-OFF LAYER; PLASMA SIMULATION; PROGRESS REPORT; RISOE NATIONAL LABORATORY; THERMONUCLEAR REACTOR MATERIALS; TURBULENCE; VORTICES

Available on request from:
Risø Library, Risø National Laboratory (Risø Bibliotek, Forskningscenter Risø)
P.O. Box 49, DK-4000 Roskilde, Denmark
Phone (+45) 46 77 46 77, ext. 4004/4005 · Telex 43 116 · Telefax (+45) 46 75 56 27

RISØ

## OBJECTIVE

**The objective of Risø National Laboratory is to further technological development in three main areas: energy, environment and materials.**

## USERS

**Risø's scientific results are widely applied in industry, agriculture and public services. Risø contributes its share of new knowledge to the global research community.**

## RESEARCH PROFILE

**Risø emphasises long-term and strategic research providing a solid scientific foundation for the technological development of society.**

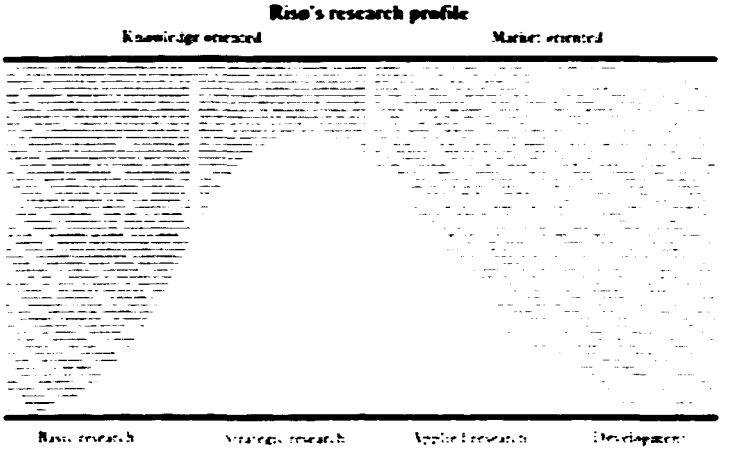


## PRIORITY AREAS

- **Combustion and gasification**
- **Wind energy**
- **Energy materials**
- **Energy and environmental planning**
- **Assessment of environmental loads**
- **Reduction of environmental loads**
- **Safety and reliability of technical systems**
- **Nuclear safety**
- **Atomic structure and properties of materials**
- **Advanced materials and materials technologies**
- **Optics and fluid dynamics**

**Risø-R-761(EN)**
**ISBN 87-550-2000-3**
**ISSN 0106-2840**

Available on request from:
**Risø Library**
**Risø National Laboratory**
P.O. Box 49, DK-4000 Roskilde, Denmark
Phone +45 46 77 46 77, ext. 4004/4005
Telex 43116, Telefax 46 75 56 27